CHAPTER 6

RADIATION BY PLATE FLEXURAL VIBRATIONS

Most underwater sound originating inside a marine vehicle is radiated by flexural vibrations of hull plates; this is especially true for frequencies above 100 Hz. The subject of plate radiation, along with the important topic of structural vibration, was first understood in Germany in the 1940's under the leadership of L. Cremer. Much of the material presented in this chapter is based on his work and that of a generation of investigators whom he influenced.

6.1 Plate Flexural Vibrations

In most recent analyses of plate flexural wave radiation the elastic equations for plate vibrations and the acoustic wave equation are treated as a system of coupled equations using solutions that are made to match at the plate surface. In this approach, the effect of the fluid is considered to be that of a load on the vibrating plate. Before considering the coupled problem, we will develop the applicable equations for plate flexural vibrations *in vacuo*.

Bending Rigidity of Plates

When classical elasticity theory is applied to solid plates, it is found that longitudinal waves have a phase speed given by

$$c_p = \sqrt{\frac{Y}{\rho(1 - \sigma^2)}} = \frac{c_Q}{\sqrt{1 - \sigma^2}} = c_s\sqrt{\frac{2}{1 - \sigma}}, \qquad (6.1)$$

as was discussed in Section 5.2. The same classical theory leads to the result that the bending rigidity of a solid plate is

$$B_p = \frac{Y\kappa^2 S}{\sqrt{1 - \sigma^2}} = \frac{Yh^3}{12\sqrt{1 - \sigma^2}} = \frac{\rho_s c_p^2 h^3}{12} \qquad (6.2)$$

per unit width. In deriving the equations for plate flexural motions from those developed for beams, these expressions replace YI wherever it occurs.

Thick Plate Bending Equations

The exact elasticity equations for bending of thick plates are very complex. A more tractable approximate equation analogous to that of Timoshenko for beams was derived by Mindlin (1951). Skudrzyk (1968) showed Mindlin's equation to be equivalent to the Timoshenko beam equation with B as given by Eq. 6.2, $\alpha' = 1$ and K related to σ by

$$K_p \doteq 0.76\left(1 + \frac{2}{5}\sigma\right) . \tag{6.3}$$

The shear parameter for plates is given by

$$\Gamma_p = \frac{Y}{KG(1 - \sigma^2)} = \frac{2}{K_p(1 - \sigma)} \doteq 2.65\left(1 + \frac{3}{5}\sigma + \frac{3}{4}\sigma^2\right) . \tag{6.4}$$

For a typical metal plate, $K_p \doteq 0.85$ and $\Gamma_p \doteq 3.3$.

With the above substitutions, the differential equation for plates corresponding to Eq. 5.26 can be written

$$\mu'\ddot{w} + \frac{\rho_s c_p^2}{12}\nabla^2 h^3 \nabla^2 w - 4.3\rho_s \frac{h^3}{12}\nabla^2\ddot{w} + \frac{3.3\mu' h^2}{12c_p^2}\ddot{\ddot{w}} = p(x,y,t) , \tag{6.5}$$

where μ' is the mass per unit area, given by $\rho_s h$. The gradient operator, ∇, replaces each derivative with respect to x, since motions propagate in two dimensions. It is assumed that changes of thickness occur relatively slowly, making spatial derivatives of thickness negligible. The bending equation corresponding to Eq. 5.28 can be written

$$\ddot{w} + \frac{c_p^2 h^2}{12}\nabla^4 w - \frac{4.3}{12}h^2\nabla^2\ddot{w} + \frac{3.3}{12}\frac{h^2}{c_p^2}\ddot{\ddot{w}} = \frac{p}{\mu'} . \tag{6.6}$$

Flexural Wave Speed

Assuming an harmonic disturbance, the homogeneous equation for flexural motions in plates can be expressed as an equation for k_i, as done for beams by Eq. 5.31. The corresponding equation is

$$\omega^2 - c_p^2\frac{h^2}{12}k_i^4 + (\Gamma_p + 1)\frac{h^2}{12}\omega^2 k_i^2 - \frac{\Gamma_p}{c_p^2}\frac{h^2}{12}\omega^4 = 0 . \tag{6.7}$$

As with the case for beams, the two real solutions for k_i represent waves and the two imaginary solutions account for distortions at discontinuities. Assuming real values for k_i, Eq. 6.7 can be transformed into an equation for the flexural wave speed,

$$\left(1 - \Gamma_p\left(\frac{\omega}{\Omega_p}\right)^2\right)\left(\frac{v_f}{c_p}\right)^4 + (\Gamma_p + 1)\left(\frac{\omega}{\Omega_p}\right)^2\left(\frac{v_f}{c_p}\right)^2 - \left(\frac{\omega}{\Omega_p}\right)^2 = 0 , \tag{6.8}$$

which corresponds to Eq. 5.35. The reference angular frequency, Ω_p, is given by

$$\Omega_p \equiv \frac{c_p\sqrt{12}}{h} . \tag{6.9}$$

At low frequencies only the first two terms of Eq. 6.7 are important, and the expression for the flexural wave speed is then similar to that given by Eqs. 5.51 and 5.53 for bars,

$$v_{f_\ell} \doteq c_p \sqrt{\frac{\omega}{\Omega_p}} = \sqrt{\frac{\omega h c_p}{\sqrt{12}}} = \frac{k_f h c_p}{\sqrt{12}} \quad . \tag{6.10}$$

The high-frequency limit for v_f is

$$v_{f_h} \doteq c_s \sqrt{K_p} \doteq 0.87 \left(1 + \frac{1}{5}\sigma\right) c_s \doteq 0.92 c_s \quad , \tag{6.11}$$

which is about 57% of the longitudinal wave speed, c_ℓ.

In the intermediate-frequency range, the flexural wave speed correction for plates is essentially the same as that for solid rectangular bars, as given by Eqs. 5.54, 5.55 and 5.56, and as plotted in Figs. 5.7 and 5.8.

Plate Vibrations

Plate vibrations are often more complex than those of beams since the motion is a function of two spatial variables. However, for relatively narrow strips the motion can be treated as straight-crested and the equations derived for beams can be used, with c_ℓ replaced by c_p. If the direction of propagation of the wave has direction cosines n_x and n_y, then

$$k_f = \sqrt{k_{f_x}^2 + k_{f_y}^2} \quad , \tag{6.12}$$

where $k_{f_x} = n_x k_f$ and $k_{f_y} = n_y k_f$. More often the plate extends in both directions and exciting forces produce motions that spread out uniformly in all directions.

Just as in Chapter 2 we treated acoustic waves from point sources in terms of symmetrical spherical waves, so we can analyze flexural waves spreading out from concentrated sources on plates as cylindrical waves in cylindrical (polar) coordinates with circular symmetry. The corresponding Laplacian in polar coordinates is

$$\nabla^2 = \frac{\partial^2}{\partial r^2} + \frac{1}{r}\frac{\partial}{\partial r} \quad , \tag{6.13}$$

and the Helmholtz form of the wave equation, Eq. 2.12, becomes

$$\frac{\partial^2 \underline{\phi}}{\partial r^2} + \frac{1}{r}\frac{\partial \underline{\phi}}{\partial r} + k^2 \underline{\phi} = 0 \quad . \tag{6.14}$$

This is a form of *Bessel's equation*, a solution of which is

$$\underline{\phi} = \underline{A} J_o(kr) \quad , \tag{6.15}$$

where J_o is a *Bessel function* of the first kind and zero order and has the shape of a damped cosine. For small values of kr,

$$J_o(kr) \doteq 1 - \left(\frac{kr}{2}\right)^2 \quad (kr << 1) \ , \tag{6.16}$$

while for very large values of the argument,

$$J_o(kr) \doteq \sqrt{\frac{2}{\pi kr}} \cos\left(kr - \frac{\pi}{4}\right) \quad (kr >> 1) \ . \tag{6.17}$$

It can be shown that the harmonic form of the plate equation is related to the Bessel equation of the form of Eq. 6.14. At low frequencies the plate equation reduces to

$$\mu' \omega^2 \underline{w} - \frac{c_p^2 \rho_s h^3}{12} \nabla^4 \underline{w} = - \underline{p} \ . \tag{6.18}$$

As in Eq. 5.59, the wave number may be expressed by

$$k_{f_o}^2 = \frac{\omega}{c_p \kappa} = \sqrt{12} \frac{\omega}{c_p h} \ . \tag{6.19}$$

Substituting for ω, Eq. 6.18 can be written

$$\mu' c_p^2 \frac{h^2}{12} \left(\nabla^4 - k_{f_o}^4\right) \underline{w} = \underline{p} \ . \tag{6.20}$$

Setting $p = 0$, the homogeneous equation can then be expressed as two simultaneous equations:

$$\left(\nabla^2 + k_{f_o}^2\right) w_1 = 0 \tag{6.21}$$

and

$$\left(\nabla^2 - k_{f_o}^2\right) w_2 = 0 \ . \tag{6.22}$$

The first of these is a Bessel equation when expressed in cylindrical coordinates and has a solution of the form of Eq. 6.15. The second has as its solution Bessel functions of imaginary arguments. It follows that w_1 and w_2 are the wave and near-field components of the displacement, w.

Dyer (1960) and Skudrzyk (1968) have shown that the homogeneous form of the Mindlin-Timoshenko thick plate equation is equivalent to three simultaneous equations. These are

$$\left(\nabla^2 + k_f^2\right) w_1 = 0 \ , \tag{6.23}$$

$$\left(\nabla^2 - \gamma^2\right) w_2 = 0 \tag{6.24}$$

and

$$\left(\nabla^2 + k_s^2\right) H = 0 \ . \tag{6.25}$$

In these equations k_f and γ are related to k_{f_o} by Eqs. 5.67 and 5.68, H is a vector potential of the shear motion in the plane of the plate, and

$$k_s^2 = K_p k_{f_o}^2 \left[2\delta_p - \frac{\Gamma_p}{2\delta_p} \right] , \tag{6.26}$$

where δ_p is defined by

$$\delta_p \equiv \frac{\Gamma_p}{2} \left(\frac{\omega}{\Omega_p} \right) = \frac{\Gamma_p}{2} \left(\frac{k_{f_o} h}{\sqrt{12}} \right)^2 \doteq \frac{1}{2} \left(\frac{k_{f_o} h}{2} \right)^2 . \tag{6.27}$$

It can be seen from the above that w_1, w_2 and H are all expressible by Bessel functions of either real or imaginary arguments.

Input Impedance

The derivation of the input impedance for a point force exciting a thin plate involves several types of Bessel functions and considerable manipulation. The approximate expression for the characteristic impedance is surprisingly simple, being

$$Z_i \doteq 8\sqrt{\mu' B_p} = \frac{4}{\sqrt{3}} \rho_s c_p h^2 = \frac{4}{\sqrt{3}} \mu' c_p h . \tag{6.28}$$

This expression, derived by Cremer (1950), is entirely real and is independent of frequency. Measurements reported by Skudrzyk et al (1961) and Snowdon (1974) of input impedances of resonant plates confirm that the characteristic impedance, as given by the geometric mean of resonant and anti-resonant minima and maxima, is in good agreement with that calculated from Eq. 6.28.

6.2 Fluid Loading

In writing the differential equations for plate flexural vibrations the forcing function was expressed as a pressure. This pressure, p, represents the sum of any applied external forcing function and the reaction on the plate of the fluid in contact with it. In this section we will consider the effect of fluid loading on a plate that experiences no other external forces.

Boundary Conditions

Fluid in contact with a plate shares the plate's motion at all points of contact. Boundary conditions are therefore the same as those considered in Section 2.5 dealing with sound transmission between two media. In this case the two media are the vibrating plate and a fluid on one side of it. The wave numbers corresponding to this vibration, k_f in the plate and k_o in the fluid, will usually be different because the speeds of waves in the two media are different. However, by Snell's law, the component of the wave number for the fluid that is parallel to the plate must match that of the flexural wave in the plate. From Eq. 2.14, the component of k_o in the plane of

the plate is

$$k_{x,y} \equiv \sqrt{k_x^2 + k_y^2} = \sqrt{k_o^2 - k_z^2} \ , \tag{6.29}$$

and this must equal k_f. It follows that

$$k_z = \sqrt{k_o^2 - k_f^2} \ . \tag{6.30}$$

Assuming straight-crested waves in the plate, any waves in the fluid will be plane waves, for which the acoustic velocity will be related to the acoustic pressure by Eq. 2.68, namely,

$$v' = \left| \vec{v}' \right| = \frac{p'}{\rho_o c_o} \ . \tag{6.31}$$

The normal component of the acoustic particle velocity must equal the velocity of the plate if the two are to remain in contact, hence

$$\dot{w} = v_z' = \frac{v_z'}{v'} \frac{p'}{\rho_o c_o} \ . \tag{6.32}$$

The ratio of the normal component to the full acoustic particle speed equals the ratio of k_z to k_o. It follows from Eqs. 6.30 and 6.32 that

$$\underline{p} = -\underline{p}' = -i\omega\rho_o c_o \frac{k_o}{\sqrt{k_o^2 - k_f^2}} \underline{w} \ , \tag{6.33}$$

which result has a number of important consequences that are dependent on the relative values of k_o and k_f.

Coincidence

When $k_o = k_f$, the fluid loading effect on flexural vibrations of an undamped plate approaches infinity. This corresponds to equality of the speeds of sound and flexural waves and was named the *coincidence effect* by Cremer (1942). As explained by Yaneske (1972), coincidence describes the maximum spatial coupling that can occur between waves in a plate and those in a fluid medium in contact with it. Actually, as noted by Kurtze and Bolt (1959), exact coincidence cannot occur since the implied infinite fluid loading would prevent the flexural wave speed from equalling that of the fluid. Nevertheless, the coincidence frequency is an important concept in dealing with plate radiation and fluid loading.

The *coincidence frequency*, f_c, is the frequency at which the flexural wave speed of a plate vibrating without fluid load would equal the sound speed in the fluid medium. For thin plates, using Eq. 6.10 for the flexural wave speed,

$$\omega_c = 2\pi f_c \doteq c_o^2 \sqrt{\frac{\mu'}{B_p}} \doteq \frac{\sqrt{12}c_o^2}{hc_p} \ . \tag{6.34}$$

The corresponding wave number is

$$k_c \doteq \sqrt{12}\,\frac{c_o}{c_p h} \quad . \tag{6.35}$$

For metal plates in air ($c_o \doteq 340$ m/sec and $c_p \doteq 5300$ m/sec),

$$f_c \doteq \frac{12}{h} \qquad (air) \ , \tag{6.36}$$

where h is the plate thickness in meters. For metal plates in water, the thick-plate intermediate-frequency correction, Eq. 5.54, must be used, and the result is

$$f_c \doteq \frac{275}{h} \qquad (water) \ , \tag{6.37}$$

At frequencies other than coincidence, flexural wave speeds are either greater or less than the speed of sound in the fluid. It is sometimes useful to express the relative speed in terms of a *flexural wave Mach number*, given by

$$M_f \equiv \frac{v_f}{c_o} = \frac{k_o}{k_f} \doteq \frac{k_f}{k_c} \doteq \sqrt{\frac{\omega}{\omega_c}} \quad , \tag{6.38}$$

where the last two relationships for coincidence wave number and frequency apply only when thin plate assumptions are valid.

Entrained Mass

Below coincidence $k_o < k_f$, and Eq. 6.33 for the pressure attributable to fluid loading becomes

$$\underline{p} = \frac{\rho_o \omega^2 \underline{w}}{\sqrt{k_f^2 - k_o^2}} \quad . \tag{6.39}$$

This has the effect of adding a second mass term to Eq. 6.18, which equation now becomes

$$\left(\mu' + \frac{\rho_o}{\sqrt{k_f^2 - k_o^2}} \right) \omega^2 \underline{w} - \frac{\mu' c_p^2 h^2}{12} \nabla^4 \underline{w} = 0 \quad . \tag{6.40}$$

Substituting for $c_p h$ from Eq. 6.19, this can be written

$$(1 + \epsilon)\underline{w} - \frac{1}{k_{f_o}^4} \nabla^4 \underline{w} = 0 \quad . \tag{6.41}$$

where ϵ is the entrained mass and is given by

$$\epsilon = \frac{\rho_o}{\mu'\sqrt{k_f^2 - k_o^2}} = \frac{\rho_o}{\rho_s k_f h\sqrt{1 - (k_o/k_f)^2}} \doteq \frac{\rho_o c_p}{\sqrt{12}\rho_s c_o} \frac{1}{M_f\sqrt{1 - M_f^2}} . \quad (6.42)$$

The relative entrained mass is thus a function of the densities and sound speeds of the two media and of the relative Mach number. Table 6.1 lists values of the media constants for aluminum and

$$\frac{\rho_o c_p}{\sqrt{12}\rho_s c_o}$$

Metal	Fluid	
	Air $\rho_o = 1.21, c_o = 340$	Water $\rho_o = 1000, c_o = 1480$
Alum. $\rho_s = 2700$, $c_p = 5400$	0.002055	0.390
Steel $\rho_s = 7800$, $c_p = 5250$	0.000692	0.1313

steel plates in air and water, and Fig. 6.1 is a plot of the Mach number dependence. The entrained mass at first decreases with increasing frequency to a minimum at $M_f \doteq 0.7$ and then increases rapidly near coincidence.

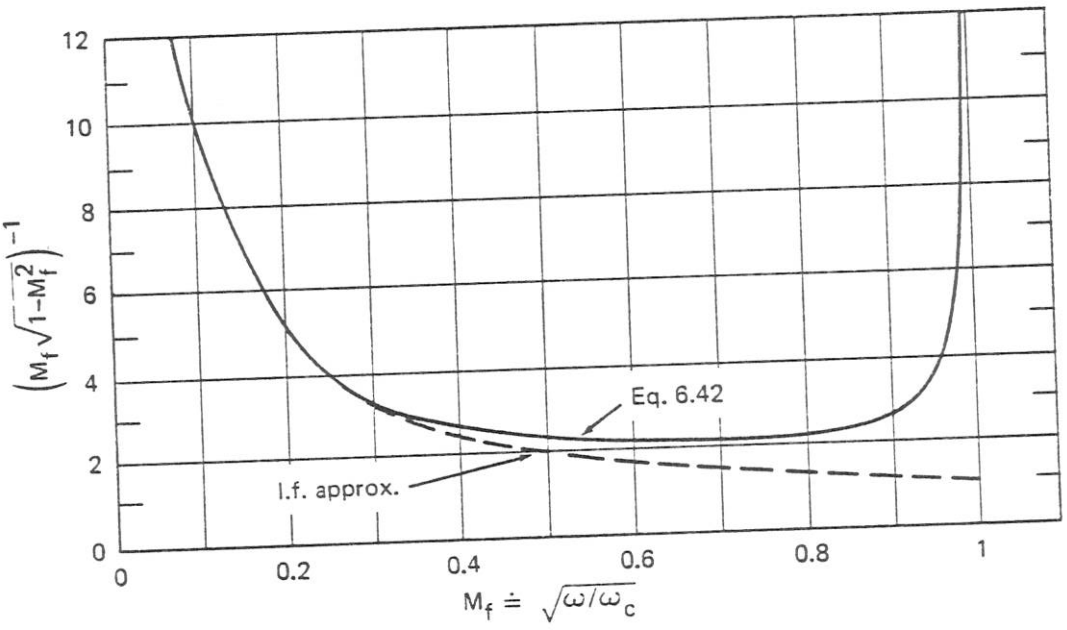

Fig. 6.1. Relative Entrained Mass Function

The entrained mass acts as a reactive load on the plate. From Eq. 4.10, the specific radiation reactance is

$$\sigma_x \equiv \frac{X_r'}{\rho_o c_o} = \frac{\mu' \epsilon \omega}{\rho_o c_o} = \frac{M_f}{\sqrt{1 - M_f^2}} , \tag{6.43}$$

which function is plotted in Fig. 6.2. Calculations of the flexural wave speed of a fluid-loaded plate should include the effects of entrained mass, as indicated in Section 5.4 for beams.

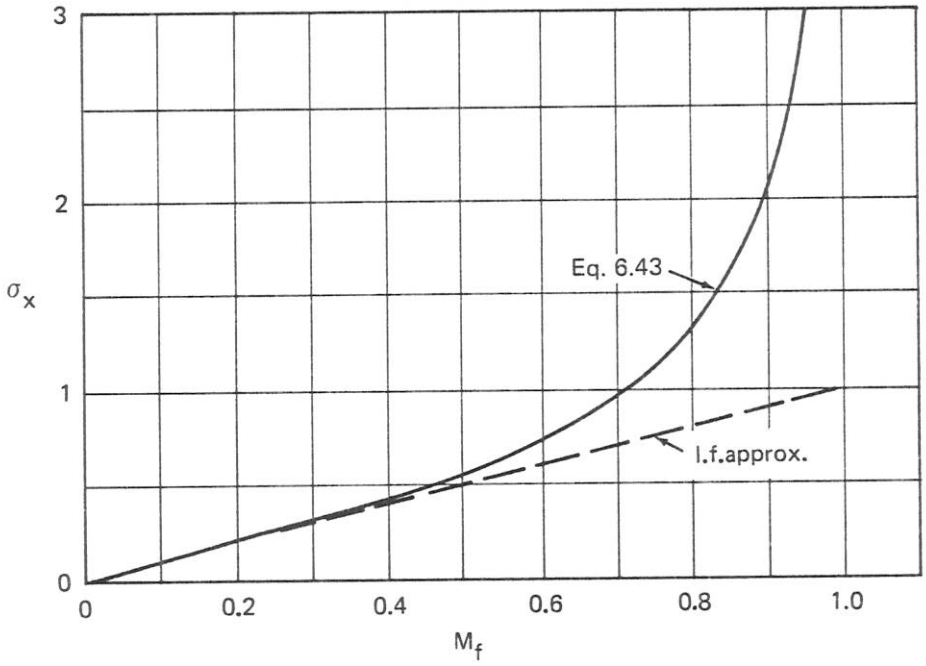

Fig. 6.2. Specific Radiation Reactance of Entrained Mass

Radiation

Above the coincidence frequency, the effect of fluid loading changes from that of an entrained mass to that of a radiation resistance and sound is radiated into the fluid. Thus, for $k_o > k_f$ the expression for the fluid pressure given by Eq. 6.33 is imaginary, representing radiation. It can be written as

$$\underline{p} = - i\omega^2 \mu' \beta \frac{M_f}{\sqrt{M_f^2 - 1}} \underline{w} , \tag{6.44}$$

where

$$\beta \equiv \frac{\rho_o c_o}{\omega \mu'} = \frac{\rho_o c_o}{\omega \rho_s h} = \left(\frac{\rho_o c_p}{\sqrt{12} \rho_s c_o} \right) \left(\frac{\omega_c'}{\omega} \right) \tag{6.45}$$

is the ratio of the specific radiation resistance of the fluid to the mass reactance of the plate per unit area. The frequency ω_c' is the low-frequency approximate value of the coincidence frequency as given by Eq. 6.34. The effect on the plate of fluid loading above coincidence is thus that of a radiation resistance. Equation 6.18 can be written

$$(1 - i\eta_r)\underline{w} - \frac{1}{k_{f_o}^4} \nabla^4 \underline{w} = 0 , \tag{6.46}$$

where

$$\eta_r = \beta \frac{M_f}{\sqrt{M_f^2 - 1}} \tag{6.47}$$

is the loss factor for sound radiation into the fluid. This function is plotted in Fig. 6.3. The motion of the plate above coincidence is damped by a loss factor, η_T, given by the sum of the radiation

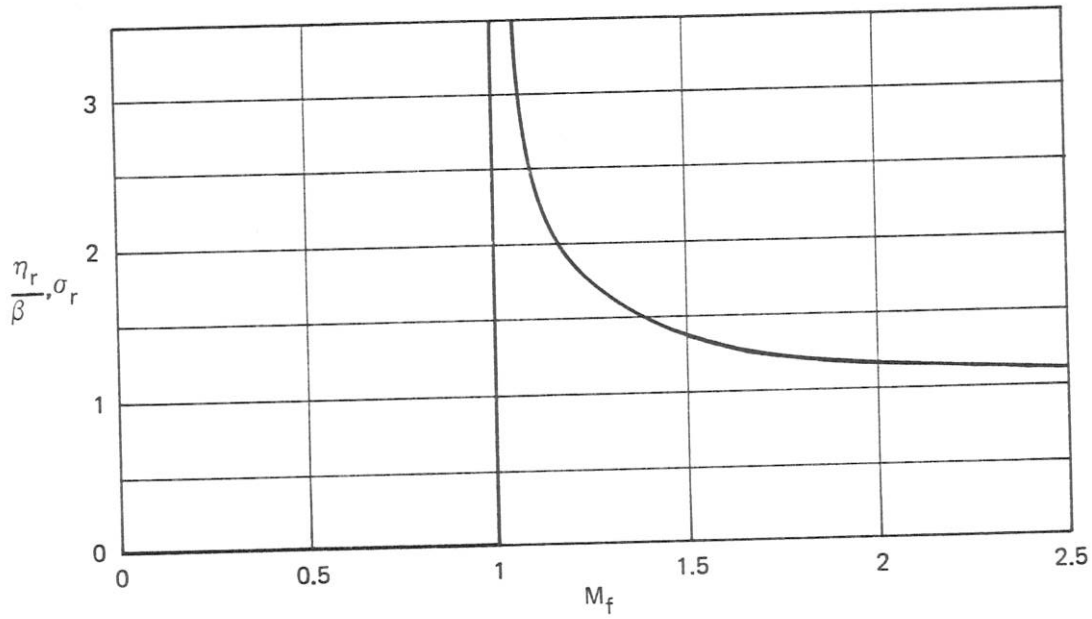

Fig. 6.3. Normalized Radiation Load Factor for Flat Plates

and structural damping loss factors. Since all power transmitted to the structure is eventually converted into sound and heat, the radiation efficiency is

$$\eta_{rad} = \frac{\eta_r}{\eta_T} = \frac{\eta_r}{\eta_r + \eta_s} . \tag{6.48}$$

Radiation only occurs at relatively high frequencies for which it usually is necessary to include shear and rotatory inertia when calculating the flexural wave speed. It follows that the approxi-

mate relations for M_f, given by Eq. 6.38, are not valid. In fact, the highest possible value of M_f is that given by using Eq. 6.11 for v_f:

$$M_{f_h} \doteq \frac{c_s\sqrt{K_p}}{c_o} \doteq 0.57\,\frac{c_\ell}{c_o} \quad . \tag{6.49}$$

The value is 8.5 for metal plates in air and only 2.0 for plates immersed in water.

As shown in Fig. 6.4, the requirement of trace matching of the acoustic and flexural waves establishes the direction of propagation of the acoustic wave. Thus,

$$\sin\theta_o = \frac{\lambda_o}{\lambda_f} = \frac{c_o}{v_f} = \frac{1}{M_f} \quad . \tag{6.50}$$

Sound waves travel parallel to the plate when $M_f \doteq 1$ and approach the perpendicular as M_f increases. The steepest angle is, of course, limited by the maximum value of M_f. Another approach to understanding Eq. 6.50 is to think of a plate with flexural waves as being composed of a line array of alternating-phase pistons spaced $\lambda_f/2$ apart. From the analysis of arrays in Section 4.7, the steered angle, θ_o, for such an array is that given by Eq. 6.50.

The angle θ_o is real only if $M_f > 1$. When $M_f < 1$, it is imaginary, corresponding to the fact that below coincidence no sound is radiated from an infinite plate and the effect of fluid loading is entirely that of added mass, as discussed above.

Returning to Eq. 6.33, the intensity of the sound radiated into the fluid can be expressed as a function of the plate velocity and the flexural Mach number by

$$I = \frac{\overline{p'^2}}{\rho_o c_o} = \rho_o c_o \frac{k_o^2}{k_o^2 - k_f^2}\,\overline{\dot{w}^2} = \rho_o c_o \overline{\dot{w}^2}\,\frac{M_f^2}{M_f^2 - 1} \quad . \tag{6.51}$$

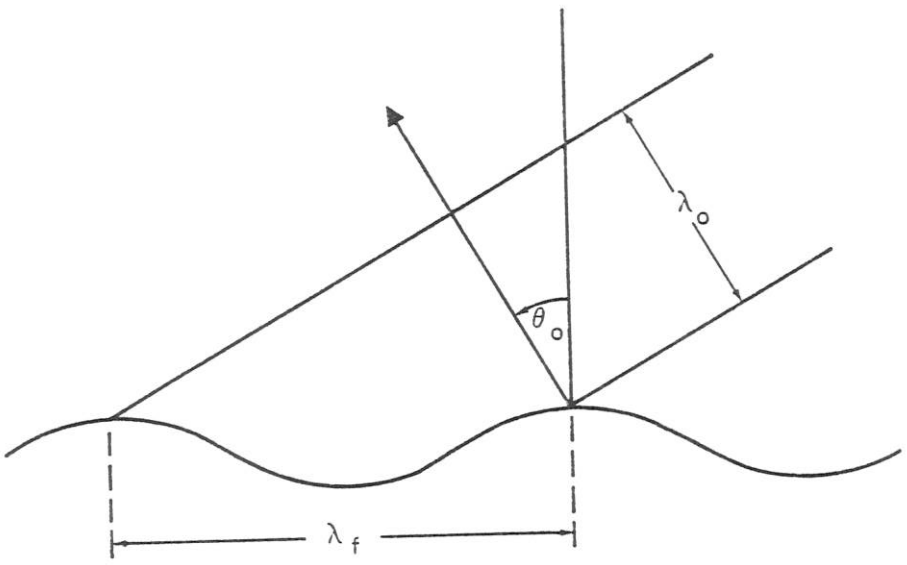

Fig. 6.4. Trace Matching of Acoustic and Flexural Waves

The power radiated per unit area of the plate is given by

$$W'_{ac} = I \cos\theta_o = \rho_o c_o \overline{\dot{w}^2} \frac{M_f}{\sqrt{M_f^2 - 1}} . \tag{6.52}$$

From Eq. 4.9, it follows that the specific radiation resistance is

$$\sigma_r = \frac{W'_{ac}}{\rho_o c_o \overline{\dot{w}^2}} = \frac{M_f}{\sqrt{M_f^2 - 1}} = \frac{1}{\cos\theta_o} , \tag{6.53}$$

and that the loss factor, η_r, equals the product of σ_r and the impedance matching function, β, i.e.,

$$\eta_r = \beta\sigma_r = \frac{\beta}{\cos\theta_o} . \tag{6.54}$$

Figure 6.3, which is a plot of η_r/β, is thus also a plot of the specific radiation resistance, σ_r. These results were first derived by Gösele (1953) and Westphal (1954).

6.3 Point-Excited Infinite Plates

The conclusion that no sound is radiated below coincidence applies only to straight-crested waves on freely vibrating infinite plates. Sound will be radiated if a plate is excited by a concentrated force. As explained in Section 6.1, flexural waves spread out equally in all directions from a point source. The solution for the velocities is in terms of Bessel functions and includes exponential near-field terms as well as wave terms. The power radiated from point-excited thin plates has been derived by Heckl (1959, 1963) and Gutin (1964) and its directional properties by Maidanik and Kerwin (1966) and Feit (1966), as well as by Gutin.

Radiation below Coincidence

For low frequencies, for which $M_f << 1$, Heckl and Gutin used Fourier transform methods to derive the radiated power, finding

$$W_{ac} = \frac{\rho_o c_o k_o^2 \overline{F^2}}{2\pi\omega^2\mu'^2} \left[1 - \beta \tan^{-1} \frac{1}{\beta} \right] , \tag{6.55}$$

where it is assumed that fluid loading occurs on one side only. The effect of fluid loading given by the term within the brackets is identical to that for piston radiation, Eq. 4.131, and is plotted in Fig. 6.5. For $\beta << 0.05$ it is essentially unity, while for $\beta > 2$ it is given by

$$1 - \beta \tan^{-1} \frac{1}{\beta} \doteq \frac{1}{3\beta^2} \qquad (\beta > 2) . \tag{6.56}$$

The two limiting cases of light and heavy fluid loading lead to significantly different results.

Light fluid loading is experienced by metal plates in air, for which $\beta < 0.05$ over most of the frequency range of interest. For this case, it is instructive to express the radiated acoustic power in

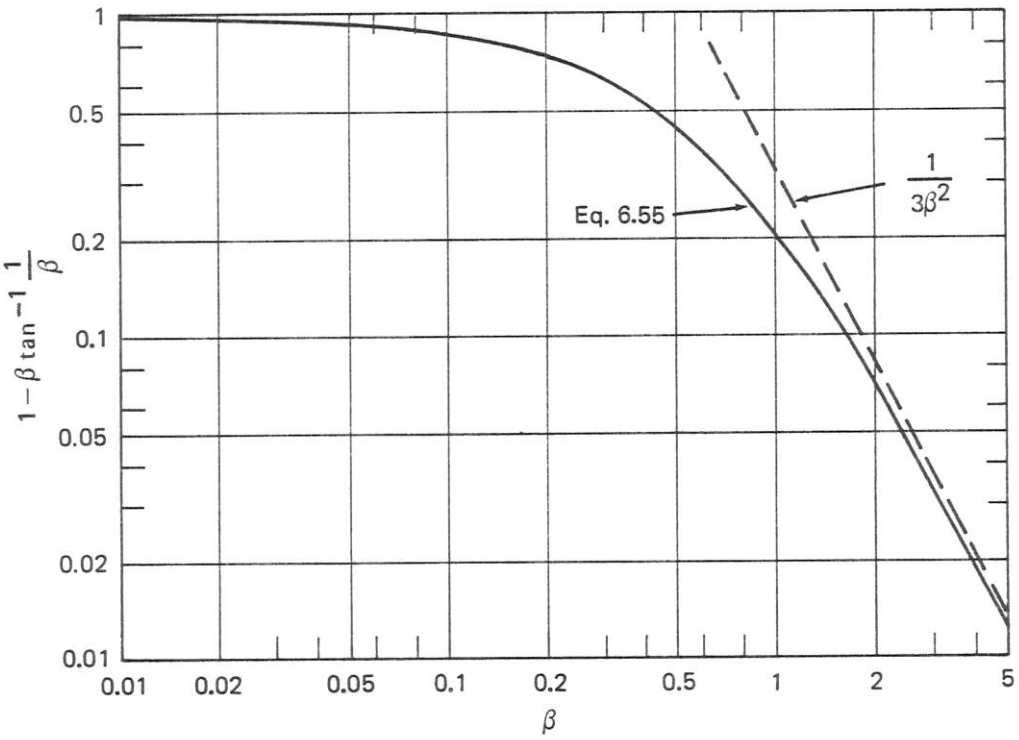

Fig. 6.5. Radiation Fluid Loading Factor, from Eq. 6.55

terms of the velocity $\dot{w}_o$ at the excitation point. Using Eq. 6.28 for the input impedance, Eq. 6.55 becomes

$$W_{ac} = \frac{32}{\pi}\rho_o c_o \frac{c_p^2 h^2}{12 c_o^2}\overline{\dot{w}_o^2} = \frac{32}{\pi}\frac{\rho_o c_o^3}{\omega_c'^2}\overline{\dot{w}_o^2} \quad . \tag{6.57}$$

Comparing this result with that for a circular piston radiating in a baffle, as given by Eq. 4.123 supplemented by Eq. 4.9, one finds

$$\frac{32}{\pi}\frac{\rho_o c_o}{k_c'^2} \doteq \frac{32}{\pi}\rho_o c_o \frac{k_o^2}{k_f^4} = \frac{\pi}{2}\rho_o c_o k_o^2 a_o^4 \quad , \tag{6.58}$$

from which it follows that the power radiated is the same as that for a circular piston of radius a_o given by

$$a_o = \sqrt{\frac{8}{\pi}}\frac{1}{k_f} = \sqrt{\frac{2}{\pi^3}}\lambda_f \doteq \frac{1}{4}\lambda_f \quad . \tag{6.59}$$

Practical sources extend over a finite area and may be treated as pistons in infinite baffles, with the piston radius being the sum of the radius of the applied force and a quarter of a flexural wavelength.

As found by Gutin (1964), Maidanik and Kerwin (1966) and Feit (1966), the radiation pattern under light loading conditions is virtually omnidirectional, the pressure at distance r being given by

$$\underline{p}'(r,\theta) \doteq \frac{\rho_o F_o}{2\pi\mu' r} e^{i(\omega t - kr)} . \tag{6.60}$$

Under these conditions the radiation efficiency is given by

$$\eta_{rad} \doteq \frac{W_{ac}}{W_{vibr}} \doteq \frac{\frac{32}{\pi} \frac{\rho_o c_o}{\omega_c'^2} \overline{\dot{w}_o^2}}{Z_i \overline{\dot{w}_o^2}} = \frac{4}{\pi} \frac{\rho_o c_p}{\sqrt{12}\rho_s c_o} . \tag{6.61}$$

This is independent of both frequency and plate thickness, being about 9×10^{-4} for steel plates in air and 2.6×10^{-3} for aluminum plates.

For metal plates in water at low frequencies, $\beta > 1$ and therefore Eq. 6.56 for *heavy fluid loading* is applicable. Equation 6.55 for the radiated sound power reduces to

$$W_{ac} \doteq \frac{k_o^2 \overline{F^2}}{6\pi\rho_o c_o} = \frac{\omega^2 \overline{F^2}}{6\pi\rho_o c_o^3} , \tag{6.62}$$

which has a cubic dependence on Mach number typical of dipole radiation. Indeed, well below coincidence the directional pattern is a cosine one. Thus, when radiating into water, a point force acting on a thin plate radiates sound at low frequencies as though the plate were not there, very much in the same manner as an oscillating hydrodynamic force, as discussed in Sections 3.4 and 9.1.

Directional Radiation at High Frequencies

Feit (1966) used the Mindlin-Timoshenko thick-plate equations in his analysis of radiation above the coincidence frequency, finding

$$\underline{p}' = \frac{ik_o F_o \cos\theta}{2\pi r} \times$$

$$\left[1 - i \frac{\cos\theta}{\beta} \frac{1 - \left(\frac{\omega}{\omega_c'}\right)^2 \left(\sin^2\theta - \left(\frac{c_o}{c_p}\right)^2\right) \left(\sin^2\theta - \Gamma_p \left(\frac{c_o}{c_p}\right)^2\right)}{1 + \left(\frac{\omega}{\omega_c'}\right)^2 \left(\frac{c_o}{c_p}\right)^2 \Gamma_p \left(\sin^2\theta - \left(\frac{c_o}{c_p}\right)^2\right)} \right]^{-1} , \tag{6.63}$$

where ω_c' is the coincidence frequency as calculated for a thin plate by Eq. 6.34. For heavy fluid loading, the second term inside the brackets is negligible and the pressure corresponds to the conditions for Eq. 6.62. On the other hand, if $\beta << 1$, as is usually true at high frequencies even in water, then Eq. 6.63 reduces to

$$p' = \frac{\rho_o F_o}{2\pi\mu' r}\left[\frac{1 + \left(\frac{\omega}{\omega_c'}\right)^2 \left(\frac{c_o}{c_p}\right)^2 \Gamma_p \left(\sin^2\theta - \left(\frac{c_o}{c_p}\right)^2\right)}{1 - \left(\frac{\omega}{\omega_c'}\right)^2 \left(\sin^2\theta - \left(\frac{c_o}{c_p}\right)^2\right)\left(\sin^2\theta - \Gamma_p\left(\frac{c_o}{c_p}\right)^2\right)}\right] \quad (6.64)$$

The function in brackets is unity when $\theta = 0$. It follows that Eq. 6.60 applies in the direction perpendicular to the plate and that the expression in brackets is the directivity function, $D(\theta)$, as defined by Eq. 4.66. Above coincidence $D(\theta)$ has a peak at the angle, θ_m, for which the denominator inside the brackets is zero, i.e., for which

$$\left(\frac{\omega_c'}{\omega}\right)^2 = \left(\sin^2\theta_m - \left(\frac{c_o}{c_p}\right)^2\right)\left(\sin^2\theta_m - \Gamma_p\left(\frac{c_o}{c_p}\right)^2\right) . \quad (6.65)$$

The lowest frequency for which the solution of this equation is real is the coincidence frequency itself, corresponding to $\theta_m = 90°$ and given by

$$\left(\frac{\omega_c'}{\omega_c}\right)^2 = \left(1 - \left(\frac{c_o}{c_p}\right)^2\right)\left(1 - \Gamma_p\left(\frac{c_o}{c_p}\right)^2\right) . \quad (6.66)$$

Putting in the constants appropriate to metal plates in water, ω_c is 21% higher than ω_c'. This is in agreement with the value derived using Eq. 5.54 and expressed by Eq. 6.37. Solutions of Eq. 6.65 for θ_m at other frequencies are in good agreement with that expected for straight-crested waves, as given by Eq. 6.50 with v_f calculated by the methods of Section 5.4. Figure 6.6 shows the angle of

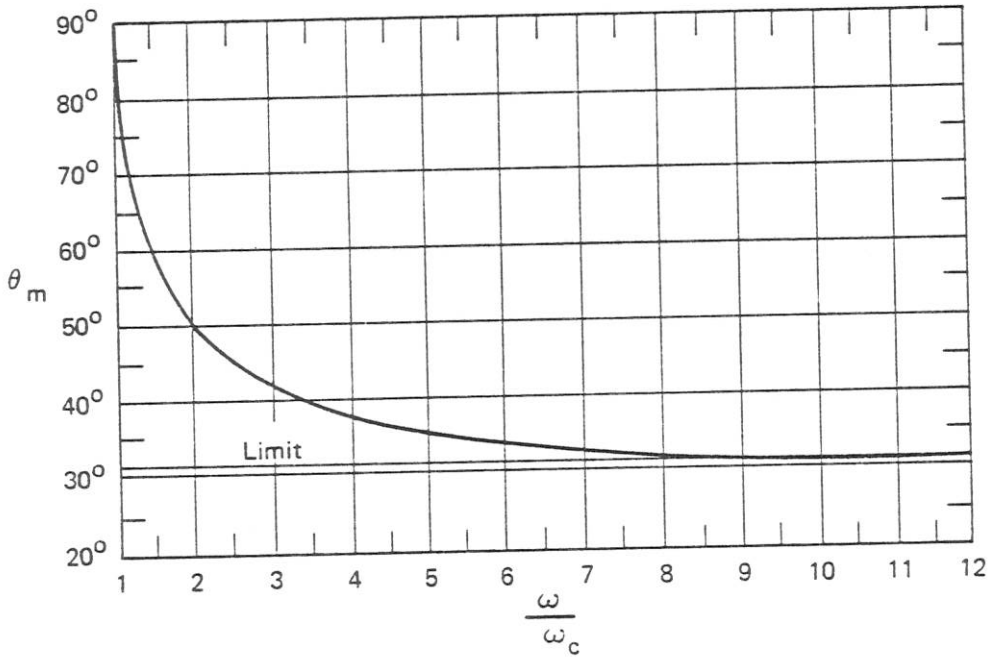

Fig. 6.6. Angle of Maximum Radiation for Metal Plates in Water, from Eq. 6.65

maximum radiation as a function of relative frequency for metal plates in water. Figure 6.7 shows a typical directional radiation pattern, as calculated by Feit. At very high frequencies, θ_m approaches the limit,

$$\sin \theta_{m_h} \doteq \frac{c_o}{v_{f_h}} = \frac{c_o}{c_p} \sqrt{\Gamma} \ , \tag{6.67}$$

which is about 31° for metal plates in water. In addition to the peak defined by Eq. 6.65, a second, smaller peak is sometimes observed at $\sin \theta_m = c_o/c_p$. This corresponds to radiation from the surface bulges associated with longitudinal plate waves. The angle for this secondary peak is about 3-2/3° in air and 16-1/2° in water.

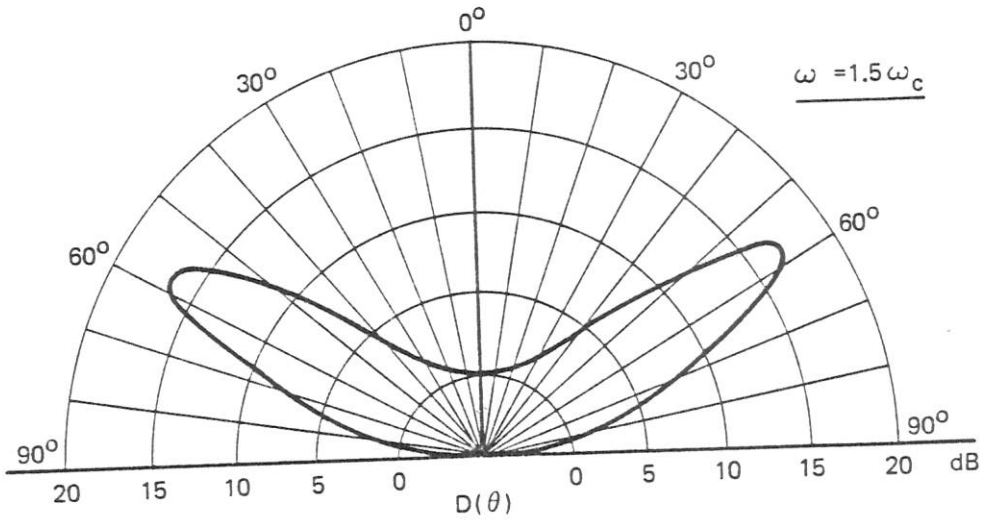

Fig. 6.7. Directional Radiation from Plate Flexural Vibrations at High Frequencies, after Feit (1966)

6.4 Radiation from Finite Plates

Radiation Resistance

The acoustic power radiated by point excitation of a very large plate below coincidence is independent of the area of the plate. For such a plate, from Eq. 4.9 for σ_r and Eq. 6.57 for W_{ac}, the specific radiation resistance for radiation into air at low frequencies is

$$\sigma_r = \frac{W_{ac}}{\rho_o c_o S \overline{w}_o^2} = \frac{32}{\pi k_c'^2 S} \doteq 0.08 \frac{\pi \lambda_c'^2}{S} \ . \tag{6.68}$$

Since λ_c' increases linearly with plate thickness, the radiation resistance for point-excited plates at low frequencies in air is proportional to the square of the plate thickness and inversely proportional to the area of the plate.

Gösele (1953, 1956) considered straight-crested standing flexural waves on baffled rectangular plates. He found

$$\overline{\sigma_r} \equiv \frac{W_{ac}}{\rho_o c_o S \overline{\dot{w}^2}} \doteq \frac{\lambda_c'}{\pi L} \qquad (M_f << 1) \ . \tag{6.69}$$

where L is the plate length in the direction of the waves as illustrated by Fig. 6.8. Nikiforov (1964) and Smith (1964) each considered finite plates with various edge conditions. They reported that

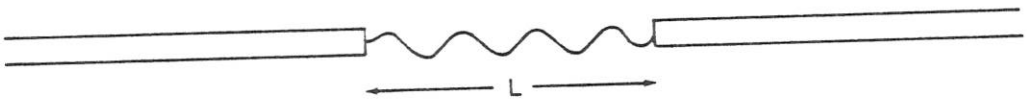

Fig. 6.8. Baffled Finite Plate with Straight-Crested Flexural Waves

clamped plates radiate most efficiently, that freely supported plates produce half as much sound and that plates with free edges radiate very little.

Gösele also considered traveling flexural waves for which the radiation efficiency is roughly half that of standing waves. His now classical plot of the radiation resistance for three relative plate lengths is reproduced in Fig. 6.9.

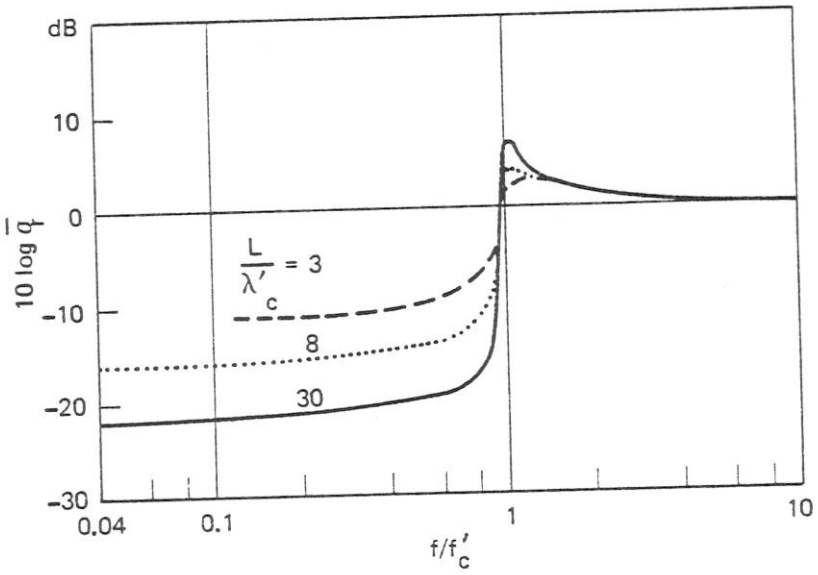

Fig. 6.9. Radiation Resistance of Traveling Waves on Finite Plates, after Gösele (1956)

Modal Approach

The general subject of radiation from plates and beam-plate systems can best be understood by following an approach to radiation problems developed by Maidanik (1962, 1974) which has received wide acceptance. As discussed in Section 5.8, finite systems have resonances which act as modes when the system is excited by an external force. All of the modes are excited to some degree. Maidanik considered all modes having flexural wavelengths shorter than that for sound waves in the fluid to be non-radiating, and those with longer wavelengths to radiate with unity efficiency. For frequencies above coincidence, most of the modes excited are radiating modes. Below coincidence, however, most of the vibratory energy is in non-radiating modes. To find the radiated power, one must calculate the fraction of the vibratory motion that is in radiating modes. Maidanik observed that below coincidence the reverberant flexural motions in the central area of a plate do not radiate and that radiation occurs only from strips at the edges that are about the width of a quarter of a flexural wavelength. Near-field pressure measurements by Blank (1968) confirm that the radiation is indeed from plate edges.

For plates that are large in both dimensions relative to a flexural wavelength but small compared to the wavelength in air, Maidanik found

$$\overline{\sigma_r} \doteq \frac{L_p \lambda_c'}{\pi^2 S} \sqrt{\frac{\omega}{\omega_c'}} = \frac{2L_p}{\pi k_c' S} \sqrt{\frac{\omega}{\omega_c'}} \quad , \tag{6.70}$$

where L_p is the plate perimeter. This relation shows a weak frequency dependence of 1.5 dB/octave, whereas that given by Eq. 6.68 for point excitation alone shows none. For a point-excited finite plate, the radiation is the sum of the forced-field component given by Eq. 6.68 and the reverberant, or edge, component given by Eq. 6.70. Before adding these two expressions, it is necessary to relate the mean-square reverberant plate velocity either to the force or to the plate velocity at the location of the force. The mean-square reverberant velocity of a flat plate can be calculated by equating the power dissipated to the vibratory power input. Thus,

$$\eta_T \omega \mu' S \overline{\overline{\dot{w}^2}} = \frac{\overline{F^2}}{Z_i} = Z_i \overline{\dot{w}_o^2} \quad , \tag{6.71}$$

where Z_i, the input impedance, is a real quantity given by Eq. 6.28. It follows that

$$\frac{\overline{\overline{\dot{w}^2}}}{\overline{\dot{w}_o^2}} \doteq \frac{8}{\eta_T k_o k_c' S} = \frac{8}{\eta_T k_f^2 S} \quad , \tag{6.72}$$

and that

$$\overline{\dot{w}^2} \doteq \frac{\overline{F^2}}{8 \eta_T \mu'^2 v_f^2 S} \quad . \tag{6.73}$$

When the reverberant contribution is added to Eq. 6.68, the result is

$$\sigma_r = \frac{W_{ac}}{\rho_o c_o S \overline{w_o^2}} \doteq 0.08 \frac{\pi \lambda_c'^2}{S} \left(1 + \frac{L_p \lambda_f}{4\pi \eta_T S} \right) . \tag{6.74}$$

When the forced radiation is added to the reverberant contribution, Eq. 6.70 becomes

$$\overline{\sigma_r} = \frac{W_{ac}}{\rho_o c_o S \overline{\dot{w}^2}} \doteq \frac{L_p \lambda_c'}{\pi^2 S} \sqrt{\frac{\omega}{\omega_c'}} \left(1 + \frac{2\eta_T k_f S}{L_p} \right) . \tag{6.75}$$

Effect of Damping

In Section 5.9 it was indicated that damping is often an effective way of accomplishing noise reduction when it is used to attenuate structural vibrations and thereby reduce the excitation transmitted to a radiating surface. Originally, however, damping materials were developed for direct application to surfaces radiating into air. While several dB of radiation reduction were usually achieved, the resultant noise reduction was always found to be much less than the vibration reduction and consequently much less than what had been expected. Nikiforov (1963) explained this relative ineffectiveness of damping by noting that below coincidence most of the vibratory energy is in short wavelength modes which are relatively easy to dampen but which do not radiate, while the radiating long wavelength modes are only slightly affected by applied damping. Examination of Eq. 6.74 leads to the same conclusion. The most that damping can do is to reduce the second term. Since even without damping this term is often smaller than unity, it is apparent that damping will usually have relatively little effect on radiation by point-excited plates below coincidence.

Orthotropic Plates

Orthotropic plates, i.e., plates having directionally dependent flexural rigidity, are useful in analyzing many practical structures, at least over part of the frequency spectrum. Heckl (1960) was the first to recognize the importance of radiation from orthotropic plates. Maidanik (1966) expressed the bending rigidity as a vector quantity. As indicated by Eq. 6.34, the coincidence frequency varies inversely with the square root of the bending rigidity, B_p. It follows that the Mach number corresponding to a given frequency is highest in the direction of maximum flexural rigidity and lowest in the direction of least rigidity. In addition, it follows from Eqs. 6.68 and 6.70 that the specific radiation resistance is also highest for radiation associated with vibrations in the direction of highest bending rigidity. Stated another way, more of the modes are of the radiating type when the bending rigidity is increased.

Feit (1970) determined that radiation patterns for orthotropic plates have a range of frequencies for which directional radiation occurs in one direction but does not occur in the perpendicular plane. This phenomenon has been confirmed experimentally in connection with radiation from cylinders.

Beam on a Plate

Beam-plate systems are quite common. The presence of a single beam attached to a plate has three distinct effects: it changes any resonance frequencies; when a vibratory force excites one region of the plate, it acts to attenuate the vibratory velocities experienced at the other side; and it increases the sound radiated by the plate.

The effect of an infinite beam attached to a plate on the propagation of straight-crested flexural waves has been analyzed by Cremer (1948) and Ungar (1961). They found that transmission occurs only at those angles for which Snell's law is satisfied for flexural waves in the plate and flexural or torsional waves in the beam. Heckl (1961) considered finite systems and found that peak transmissions occur at frequencies close to beam resonance frequencies. For relatively high frequencies and long beams, Heckl found the broadband average transmission coefficient to be given by

$$\alpha_t^2 = \frac{\overline{\overline{v_2^2}}}{\overline{\overline{v_1^2}}} \doteq \frac{k_B \mu_p'}{k_p^2 \mu_B} \left(1 + 64 \frac{\mu_p'}{k_p \mu_B} \right) , \tag{6.76}$$

where subscript p refers to plate and subscript B to beam. The second term in Eq. 6.76 is negligible for heavy beams but important for relatively light ones. Heckl measured transmission through a 2.5 cm high steel beam on an 0.8 mm thick aluminum plate in air, finding transmission loss values of from 15 to 35 dB. Without including beam resonances in his analysis, Nikiforov (1969) showed that Eq. 6.76 can be derived by considering the transmission of diffuse fields by infinite beam-plate systems.

The attenuation of flexural waves by a beam or other obstacle may be reduced significantly if the plate is immersed in liquid. Lyapunov (1968) has shown that an appreciable fraction of the incident energy may be transferred past the obstacle by the near-field acoustic disturbance in the liquid.

As for sound radiation, Maidanik (1962), Lyon (1962) and Romanov (1971) have all shown that the presence of a beam can significantly increase plate radiation below coincidence. Maidanik established that beams have the effect of increasing the ratio of perimeter length to surface area, thereby increasing the contribution from the reverberant field, as implied by Eq. 6.70. Lyon evaluated the radiation resistance per unit length of beam for a number of assumed boundary conditions and found that

$$R_r' \doteq 0.6 \rho_o h_p c_Q M_f \tag{6.77}$$

at low frequencies, with only slight dependence on boundary assumptions. Romanov noted that the increase in radiation occurs if plate damping is small, but that heavy damping, $\eta > 0.1$, can negate the effect of the beam. It thus appears valuable to apply damping to plates for which attached beams would otherwise result in increased radiation.

Periodic Structures

Heckl (1961) examined plates with periodically-spaced beams both experimentally and theoretically. He found that the first of a series of beams has the greatest effect on vibration transmission. The first beam only passes waves which approach it at angles such that there is wave number matching between the incident waves and waves propagating in the beam. Since these angles are also the correct ones to pass the second beam, only scattering within the bays will result in additional attenuation by the second and subsequent beams. Heckl confirmed this understanding by showing experimentally that varying the spacing of identical beams has little effect but that varying the shape of one beam has significant effect. Thus, beams on plates can be considered to be filters which pass flexural waves having certain propagation directions and frequencies.

Putting identical filters in series adds little attenuation in their pass band. Variation of filter characteristics is much more effective in reducing transmission.

Maidanik (1962) and Plakhov (1967) found that periodically-spaced ribs increase the radiation from a plate by from 6 to 12 dB, the higher values being measured for plates radiating into air and lower ones being more typical of water loading. The theoretical expressions derived by both investigators are quite complex and imply considerable variability of the effect of multiple beams on sound radiation.

At very low frequencies, for which the spacing between beams becomes short compared to a flexural wavelength, the beams no longer act as periodic impedance elements. Instead they act to distribute stiffness in the parallel direction and add mass in the perpendicular direction. Thus, at very low frequencies periodic structures behave acoustically as orthotropic plates with the directional radiation characteristics previously discussed.

Cylindrical Shells

The dominant effect of plate curvature is to add stiffness without adding mass. Thus, conclusions reached in our discussion of orthotropic plates apply to curved plates and are also indicative of properties of cylindrical shells. The parameter that expresses the relative importance of plate curvature is

$$\nu \equiv \frac{\omega a}{c_p} \text{ , or } \frac{\omega a}{c_\ell} \text{ ,} \tag{6.78}$$

where a is the radius of curvature. If $\nu < 1$, curvature affects both vibrations and radiation significantly. On the other hand, for $\nu > 2$, curved surfaces behave as flat plates. Heckl (1962) calculated modal densities of cylindrical shells by using an approximate formula for resonance frequencies,

$$\nu_{m,n} \doteq \frac{(m\pi a/L)^2}{n^2 + (m\pi a/L)^2} + \frac{h}{\sqrt{12}a}\left(n^2 + (m\pi a/L)^2\right) \text{ ,} \tag{6.79}$$

where m is the number of longitudinal modes, n the number of circumferential ones, and a, L and h are the radius, length and thickness of the shell. Heckl found that for $\nu < 1$ there are approximately $\sqrt{\nu}$ as many resonances per frequency band as there would be for a flat plate. He also showed that low-order longitudinal modes of cylindrical shells have much higher flexural wave speeds than do those of flat plates. Manning and Maidanik (1964) measured the acoustic power radiated by a point-driven cylindrical shell in air. As shown in Fig. 6.10, they found that below coincidence the radiation resistance decreases at a rate of about 6 dB/octave until it reaches the value attributable to the force alone. Similar results were found by Szechenyi (1971).

As noted by Komarova (1969), applied damping is less effective in reducing radiation from cylinders than from plates. As she explained, most of the vibratory energy is in circumferential modes which, though readily damped, do not radiate efficiently. Radiation is dominated by the relatively stiff longitudinal modes which have higher flexural wave speeds and which are also harder to damp.

Radiation from Hull Sections

Although curved plates and reinforcing ribs make hull structures quite complex, the discussion of orthotropic plates and cylindrical shells given thus far in this section indicates that general

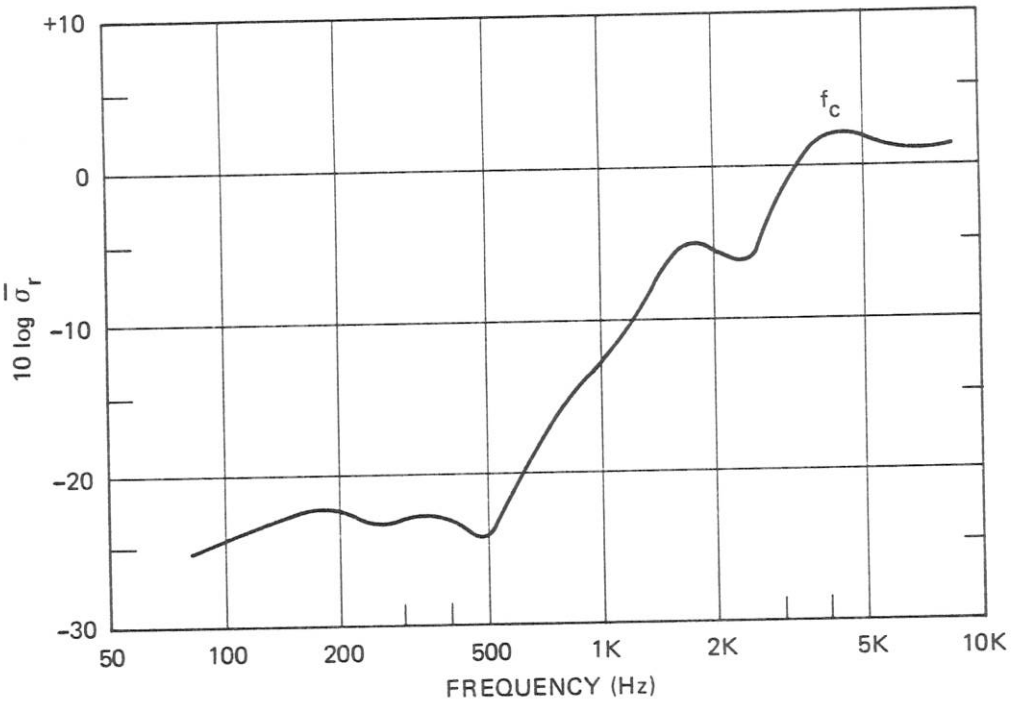

Fig. 6.10. Radiation from a Cylinder in Air, after Manning and Maidanik (1964)

characteristics of hull radiation can be predicted from rather elementary formulas. Thus, Eq. 6.62 can be used at low frequencies for which water loading is significant. This can be written:

$$W_{ac} \doteq \frac{\omega_c'^2 F^2}{\rho_o c_o^3} \frac{M_f^4}{6\pi} \qquad (M_f << 1) \ . \tag{6.80}$$

At high frequencies essentially all of the vibratory power accepted by the structure will be radiated. Thus,

$$W_{ac} \doteq \frac{\overline{F^2}}{Z_i} \doteq \frac{1}{8} \frac{\omega_c'^2 \overline{F^2}}{\rho_o c_o^3} \left(\frac{\rho_o c_p}{\sqrt{12}\rho_s c_o} \right) \qquad (M_f > 1) \ , \tag{6.81}$$

where the factor in parentheses is given in Table 6.1. The result of combining Eqs. 6.80 and 6.81 is shown in Fig. 6.11 for aluminum and steel plates in water. This ignores any reverberant contribution.

Donaldson (1968) measured the radiated power for several ship-like structures floating in a tank of water, finding good agreement with Fig. 6.11 for frequencies above about 400 Hz, corresponding in his case to $\omega/\omega_c' \doteq 0.02$. Below this frequency, the measured power exceeds the calculated power by an increasing amount. At the low frequencies, resonances are prominent and reverberant energy is apparently dominant. Donaldson's low-frequency results correspond to a radiation factor, as given by Fig. 6.11, of about - 45 dB. Thus his results are consistent with those of Fig. 6.11 provided a minimum floor of about - 45 dB is used for the lowest frequencies.

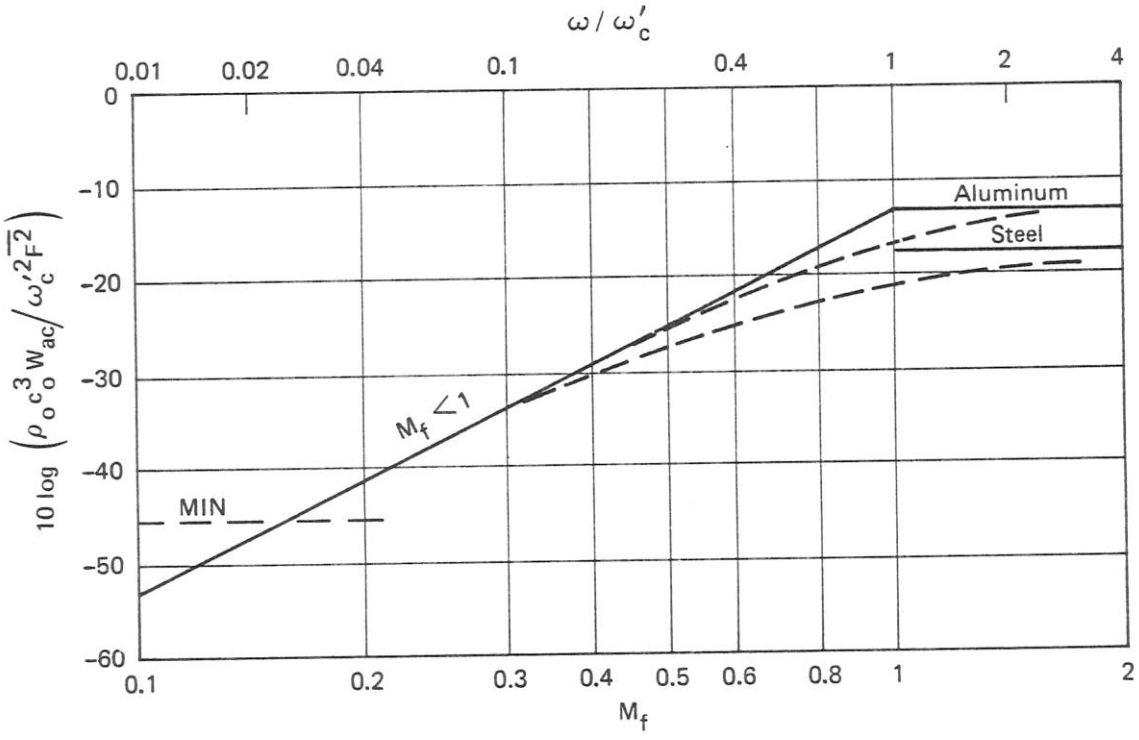

Fig. 6.11. Sound Radiation by Forces Applied to Flat Plates in Water

Equations 6.80 and 6.81 combined with Eq. 6.34 for ω_c' indicate that hull construction plays a relatively minor role in governing the acoustic power radiated by a given force. In the mid-frequency range for which Eq. 6.80 applies the power radiated is independent of hull parameters. At high frequencies, above the coincidence frequency, less sound is radiated the thicker the hull and the lower the value of ω_c'. Steel radiates a few dB less than aluminum. No conclusions can be stated for the lowest frequencies since Donaldson's tests did not cover a wide range of plate thicknesses. The reverberant field is important at these frequencies and structural details may be expected to affect the amount of sound radiated at specific frequencies.

6.5 Transmission through Structures

A common situation in acoustics is that in which sound waves in one body of fluid are transmitted into a second fluid separated from it by a solid structure. In a sonar dome the aim is to minimize any effects of the structure. In other cases maximum transmission loss may be desired.

Response of Structures to Sound Waves

The response of structures to incident sound waves is the inverse of the problem of radiation of sound by structures. Lyamshev (1959) noted that the *acoustic reciprocity principle*, whereby sources and receivers are interchangeable, applies equally well to structural radiation situations. Thus, the velocity of a plate structure that is excited by a uniformly distributed sound field is directly related to the sound field radiated by the same structure when excited by a point force.

The radiation resistance coefficients derived in the previous section are therefore indicative of the sound-absorbing properties of structures. Sound excites radiative long wavelength modes and does not excite non-radiative short modes. Thus, above coincidence flexural waves are readily excited by sound, but below coincidence their response is relatively weak.

Low-Frequency Transmission through Walls

Below the coincidence frequency, the dominant mechanism of sound transmission through plates and walls is that involving longitudinal waves. Consider the situation depicted in Fig. 6.12 in which fluid body 1 is separated from fluid body 2 by a solid wall of thickness h, which is thin

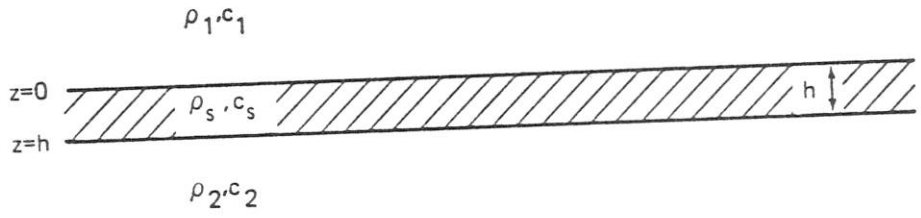

Fig. 6.12. Wall Separating Two Fluids

compared to a wavelength in the solid. The two fluids may be the same or different. It is assumed that both density and sound speed are higher in the structure than in the fluid. Application of Snell's law at both interfaces, taking into account phase shifts as well as amplitudes, results in

$$\alpha_t \equiv \frac{I_t}{I_i} = \frac{\overline{p_2^2}}{\rho_2 c_2} \Bigg/ \frac{\overline{p_1^2}}{\rho_1 c_1} \doteq \frac{4\rho_2 c_2 \rho_1 c_1}{(\rho_2 c_2 + \rho_1 c_1)^2 + (\rho_s h\omega)^2} \tag{6.82}$$

for normal incidence. Taking the reciprocal, and noting that $\rho_s h$ equals the surface density μ', it follows that

$$\frac{1}{\alpha_t} = \frac{1}{4}\left(2 + \frac{\rho_1 c_1}{\rho_2 c_2} + \frac{\rho_2 c_2}{\rho_1 c_1} + \frac{\mu'\omega}{\rho_1 c_1} \cdot \frac{\mu'\omega}{\rho_2 c_2}\right), \tag{6.83}$$

and the *transmission loss*, TL, is $10 \log \alpha_t^{-1}$. There are several special cases of interest:

1. *Water to water*. The two fluids are identical and Eq. 6.83 reduces to

$$\frac{1}{\alpha_t} = 1 + \frac{1}{(2\beta)^2}. \tag{6.84}$$

where β is the load factor defined by Eq. 6.45. The resultant TL is plotted in Fig. 6.13, where it is seen that the loss is less than 3 dB provided $f < 1/4\, f_c$.

2. *Air to air*. Equation 6.84 applies and β is very small. Hence,

$$TL \doteq 20 \log \frac{\mu'\omega}{2\rho_o c_o}. \tag{6.85}$$

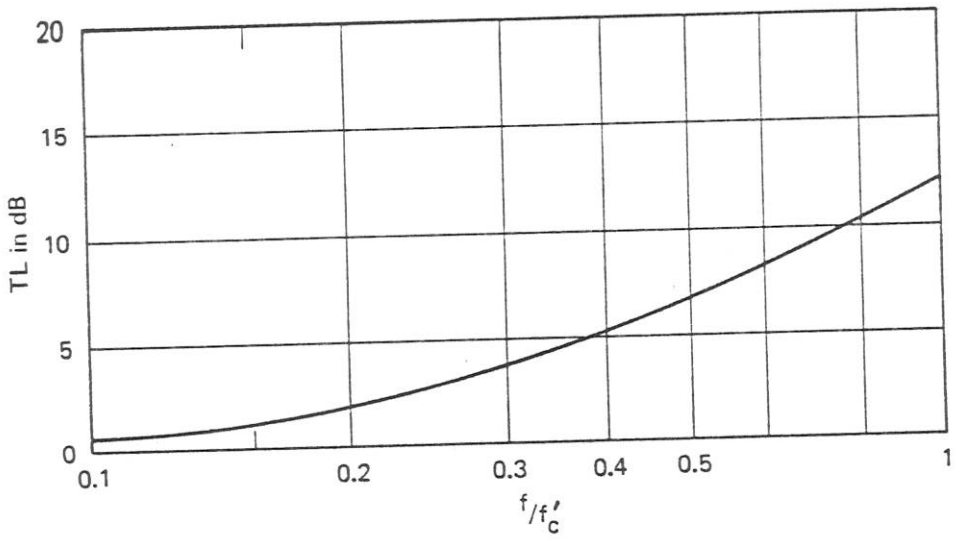

Fig. 6.13. Ideal Transmission Loss for Steel Plates in Water, from Eq. 6.84

The transmission loss increases with frequency and with structural density. This is the familiar *mass law* that governs transmission by walls at low frequencies up to about $1/2\, f_c$.

3. *Water to air.* In this case $\rho_1 c_1 >> \rho_2 c_2$, and Eq. 6.83 reduces to

$$\frac{1}{\alpha_t} \doteq \frac{\rho_1 c_1}{4\rho_2 c_2}\left(1 + \frac{1}{\beta_1^2}\right) . \tag{6.86}$$

Since $\beta_1 > 1$ for water loading at low frequencies, this result differs very little from that derived in Section 2.5. Thus, well below coincidence the solid structure has no effect on the transmission loss. Only for $f > 1/5\, f_c$ does it reduce the power transmitted.

4. *Air to water.* In this case $\rho_1 c_1 << \rho_2 c_2$, and Eq. 6.83 reduces to

$$\frac{1}{\alpha_t} = \frac{\rho_2 c_2}{4\rho_1 c_1}\left(1 + \frac{1}{\beta_2^2}\right) . \tag{6.87}$$

Since water is now the second medium, the result is identical to that for water to air, in conformity with the reciprocity theorem.

It is clear from these four examples that the structure plays a relatively minor role below coincidence if water loading occurs on one or both sides. Only in the air-to-air case can a large TL be achieved in the low-frequency regime.

Use of Impedance Concepts

The equations for normal-incidence transmission loss at low frequencies can readily be extended to other angles of incidence and other types of wave motions in the structure by using relatively elementary network concepts. In this approach, each medium is characterized by one or

more impedance elements in series or in parallel and these elements are placed in series with each other. The power transmission coefficient, α_t, is the ratio of the power transmitted through the intervening structure to that which would have been transmitted if the structure were absent and medium 2 were identical to medium 1. Consider the circuit shown in Fig. 6.14. The power

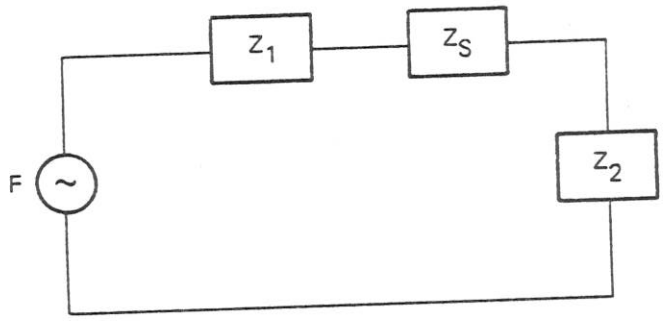

Fig. 6.14. Network Representing Transmission Loss

delivered to the load, Z_2, is

$$W_2 = \frac{R_2\overline{F^2}}{\left|\underline{Z}_1 + \underline{Z}_2 + \underline{Z}_s\right|^2} = \frac{R_2\overline{F^2}}{(R_1 + R_2 + R_s)^2 + (X_1 + X_2 + X_s)^2} . \quad (6.88)$$

If $Z_s = 0$ and $\underline{Z}_2 = \underline{Z}_1 = R_1$, then

$$W_2^0 = \frac{R_1\overline{F^2}}{(2R_1)^2} = \frac{\overline{F^2}}{4R_1} . \quad (6.89)$$

It follows that

$$\alpha_t \equiv \frac{W_2}{W_2^0} = \frac{4R_1R_2}{(R_1 + R_2 + R_s)^2 + (X_1 + X_2 + X_s)^2} . \quad (6.90)$$

At a surface, the normal impedance for longitudinal waves in a fluid medium is given by

$$\underline{Z}_i = \frac{\rho_i c_i S}{\cos\theta_i} , \quad (6.91)$$

which is purely resistive. At frequencies sufficiently below coincidence, walls can be treated as masses for which $\underline{Z}_s = i\omega m = i\omega\mu' S$. Substituting these relations into Eq. 6.90 and assuming normal incidence, Eq. 6.83 can be derived for the transmission coefficient. For oblique incidence, each ρc product should be replaced by $\rho c/\cos\theta$, where θ is the angle relative to the normal.

Role of Flexural Vibrations

As discussed by Beranek (1959) and Schiller (1967), flexural waves become dominant in wall transmission for frequencies above about $1/2\, f_c'$. Those components of a diffuse sound field that match the reverberant wave field of the structure are transmitted virtually without loss. The remainder is reflected. The reverberant velocity of the structure is controlled by the damping

factor as given by Eq. 6.73. Cremer, Heckl and Ungar (1973) used reciprocity to show that the radiation process is related to the absorption process by $k_o^2 S/4\pi$. They found that the effective wall impedance, $\underline{Z}_s$, for flexural waves above coincidence is a pure resistance given by

$$R_s^2 = \frac{k_o^2}{4\pi} \eta_T \omega \mu' Z_i S^2 = \frac{2}{\pi} k_o^2 \mu'^2 \eta_T v_f^2 S^2 \doteq \frac{2\eta_T}{\pi} \left(\frac{\omega}{\omega_c'} \right) (\omega \mu' S)^2 \quad . \tag{6.92}$$

This resistance is relatively small when either fluid is a liquid, but is significant when both fluids are gases. Thus, for air-to-air transmission, substitution of Eq. 6.92 into Eq. 6.90 leads to

$$TL \doteq 10 \log \frac{R_s^2}{4R_1 R_2} \doteq 20 \log \frac{\omega \mu'}{2\rho_o c_o} + 10 \log \frac{2\eta_T}{\pi} + 10 \log \frac{\omega}{\omega_c'} \quad . \tag{6.93}$$

The first term is the mass law of Eq. 6.85, the second term is negative by an amount that depends on total damping and the third term is an additional dependence on frequency. It is apparent that, for frequencies controlled by flexural wave transmission, the amount of isolation that can be achieved by built-in damping is second only to that caused by the wall's mass.

Sound Isolation by Walls

When walls are being used to isolate one space from another acoustically, several things can be done to decrease the transmission. The most obvious is to raise the coincidence frequency above the frequency range for which high TL is desired. This poses a problem in that f_c is inversely dependent on thickness and TL in the mass law regime is proportional to thickness. Kurtze (1959) and Kurtze and Watters (1959) proposed that the flexural wave speed be reduced without sacrificing mass by using multilayered plates in which a viscous liquid, a viscoelastic solid or a porous layer is placed between two thin elastic layers. A number of practical wall constructions have been developed using this principle.

It has been demonstrated that anything adding stiffness to a wall without adding much mass is detrimental to sound isolation. Venzke et al (1973) demonstrated that adding stiffeners to walls increases their sound radiation below coincidence and thereby decreases the TL. Shenderov (1963, 1969), Plakov (1968) and Warren (1974) demonstrated that periodically-spaced stiffeners on plates cause rejection bands for which the TL is high as well as pass bands for which it is low. Shenderov (1964) proved theoretically what a large number of investigators have found experimentally, namely, that the method of support of a panel affects its acoustic transmissivity.

It is clear that, at coincidence as well as above it, the TL of a wall is a direct function of its damping. Increasing the damping is probably the single most effective way of increasing TL in cases where it is impossible to use *limp* walls that have both high mass and low stiffness, i.e., low flexural wave speeds together with high surface mass densities.

6.6 Boundary-Layer Flow Noise

When fluid flows past a surface, a boundary layer is formed in which the flow velocity decreases from a value related to the free-stream velocity to zero at the surface. Often the boundary layer is characterized by turbulent flow conditions involving fluctuating velocities and pressures. The radiated and sonar self-noise associated with such turbulent pressure fluctuations is called *boundary-layer flow noise*. Although this topic has interested many investigators over the

past 20 years, full understanding of all of the noise-generating mechanisms is still lacking. This section begins with a description of the significant characteristics of turbulent boundary-layer flows based primarily on papers published by the author.

Turbulent Boundary Layers

If a fluid were completely inviscid, it would theoretically be able to flow past a surface with finite relative speed. However, even a small amount of viscous friction is sufficient to cause zero local flow speed right at the surface. The transition region from the surface to the point where viscosity has no effect is termed the *boundary layer*. Close to the nose of a body, or in pipes at very low flow speeds, fluid viscosity dominates and the boundary layer is laminar. However, further downstream and/or at higher flow speeds the laminar shear layer becomes unstable and eddies form. These eddies become dominant and eddy momentum transfer becomes more important than viscous transfer as the boundary layer becomes turbulent. Since flow fluctuations associated with laminar flows are very small, laminar boundary-layer flow noise is negligible. It is the eddy motions of turbulent boundary layers that give rise to velocity and pressure fluctuations and thereby cause flow noise. Hence, all discussions of boundary-layer flow noise refer to the turbulent condition.

The physical quantities which characterize a *turbulent boundary layer* are the mean flow velocity distribution, $u(z)$, and the distributions of turbulent stresses, $\tau(z)$, eddy mixing lengths, $\ell(z)$, and turbulent velocity components, u', v' and w'. The thickness of the disturbed layer, δ, is an indefinite quantity and it is common practice to describe the extent of the layer by the *displacement thickness*, δ^*, defined by

$$\delta^* \equiv \int_0^\infty \left(1 - \frac{u}{u_1} \right) dz \ , \tag{6.94}$$

and/or the *momentum thickness*, θ, given by

$$\theta \equiv \int_0^\infty \left(1 - \frac{u}{u_1} \right) \frac{u}{u_1} \, dz \ , \tag{6.95}$$

where u_1 is the flow velocity immediately outside the disturbed region. The displacement thickness measures the extent by which the ideal potential flow streamlines are displaced from the surface by the boundary layer, while the momentum thickness measures the momentum deficiency.

Figure 6.15 shows several typical turbulent boundary-layer velocity profiles. Each boundary layer consists of two basically different major regions, called inner and outer. The *inner region* is controlled by local wall conditions and the *outer region* is dominated by eddies that were created relatively far upstream. As shown in Fig. 6.16, a *blending region* connects the two. The inner region is further divided into three zones: a *laminar sublayer* in immediate contact with the wall in which the turbulence level is low and viscosity dominates, a *buffer zone* in which viscous and turbulent shear stresses are both active, and a *turbulent zone* in which the level of turbulence is governed by local wall conditions.

The velocity distribution in the *inner region* is related to the value of the shear stress at the

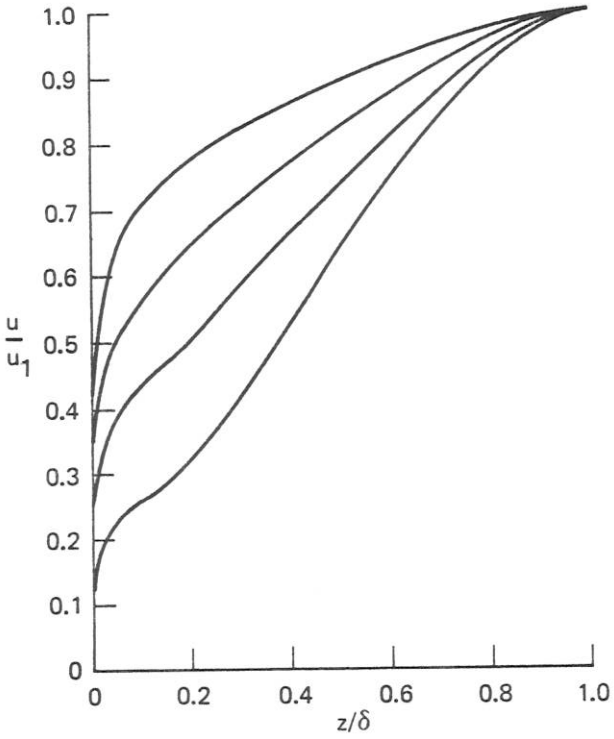

Fig. 6.15. Four Typical Turbulent Boundary-Layer Velocity Profiles, from Ross (1956)

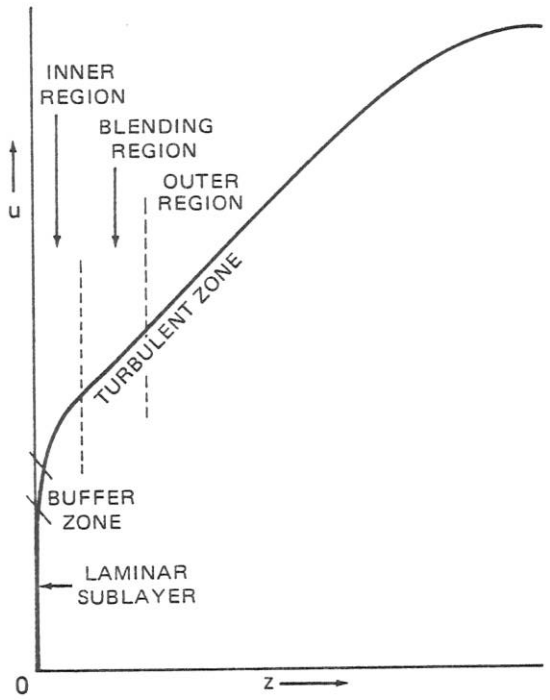

Fig. 6.16. Regions of a Turbulent Boundary-Layer Velocity Profile, from Ross (1956)

wall, τ_w. This is usually expressed by a velocity, u_τ^*, called the *friction velocity*, or wall-shear-stress velocity, defined by

$$u_\tau^* \equiv \sqrt{\frac{\tau_w}{\rho_o}} \quad . \tag{6.96}$$

The inner velocity profile is a function of the *non-dimensional distance* from the wall,

$$z_\tau \equiv \frac{z u_\tau^*}{\nu} \quad , \tag{6.97}$$

and the relative wall roughness. In the *laminar sublayer* adjacent to a smooth wall,

$$\frac{u}{u_\tau^*} = z_\tau \quad . \tag{6.98}$$

As shown in Fig. 6.17, this linear region extends only as far as $z_\tau \doteq 5$. Beyond $z_\tau \doteq 20$ and extending outward for about 10% of the total boundary-layer thickness the velocity profile is

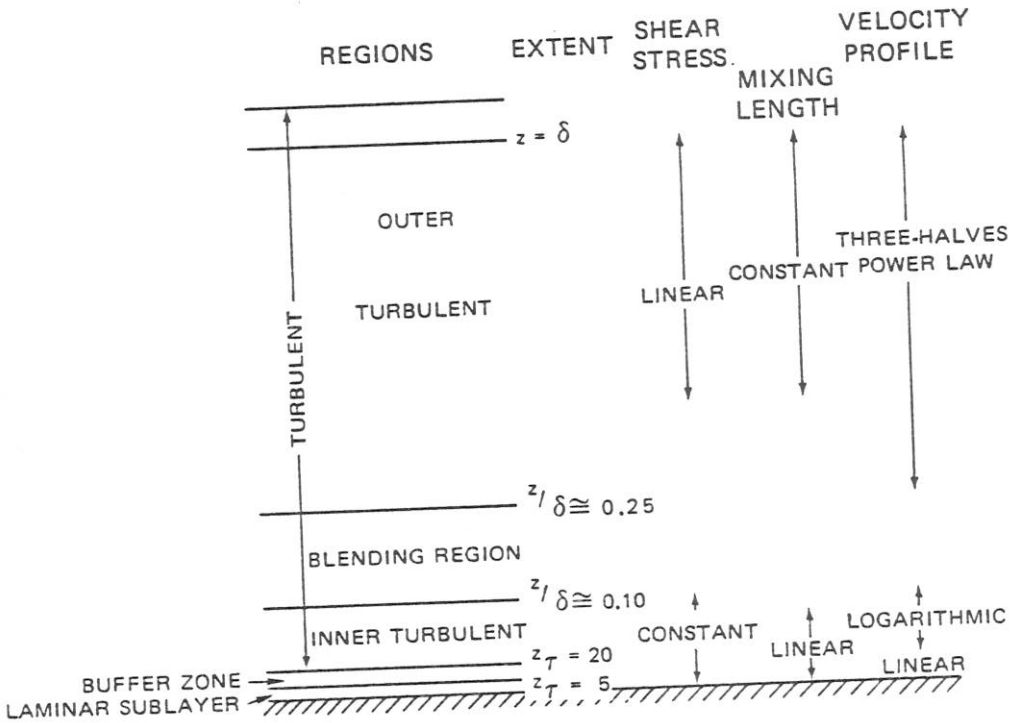

Fig. 6.17. Properties of the Regions of a Smooth-Wall Turbulent Boundary Layer, from Ross (1956)

logarithmic, of the form

$$\frac{u}{u_\tau^*} = A + B \log z_\tau \quad . \tag{6.99}$$

For smooth walls, both constants are approximately 5.6. That these coefficients are practically universal constants independent of pressure gradients, Reynolds number and upstream history was first proposed by Ludwieg (1949) and is known as the *law of the wall*. For smooth walls, the log-law relation of Eq. 6.99 intersects the linear relation of Eq. 6.98 at $u_\tau^* \doteq 11.5$.

As shown in Fig. 6.17, the *outer turbulent region* is characterized by having essentially constant eddy mixing length. Its velocity distribution is a defect relation in which the velocity is expressed relative to its undisturbed value by

$$\frac{u}{u_1} = 1 - f\left(\frac{z}{\delta}\right) \quad . \tag{6.100}$$

That the magnitude of the velocity defect should be a function of upstream rather than local conditions was proposed by Prandtl (1935) and by Schultz-Grunow (1938). Ross and Robertson (1950) demonstrated that this fact is central to an understanding of boundary-layer phenomena. They called the dependence of the outer profile on upstream conditions the *history effect*, and Coles (1956) later named it the *law of the wake*. The outer profile can be expressed as a power function of the distance inward from the outer edge of the layer, namely

$$\left(1 - \frac{u}{u_1}\right) \sim \left(1 - \frac{z}{\delta}\right)^n \quad . \tag{6.101}$$

Ross (1956) chose $n = 1.5$, writing

$$\frac{u}{u_1} = 1 - D\left(1 - \frac{z}{\delta}\right)^{3/2} \quad ; \tag{6.102}$$

other investigators have found better fits to their data using somewhat different values of the exponent. The critical point is that the outer region in all cases is a defect region in which the magnitude of the velocity deficiency and its shape are determined by upstream conditions.

The inner and outer profiles connect in the *blending region*. As shown in Fig. 6.15, this may involve an inflection point. In the blending region both local wall conditions and spatial history are important and no simple velocity profile has been proposed. Figure 6.18 shows how inner and

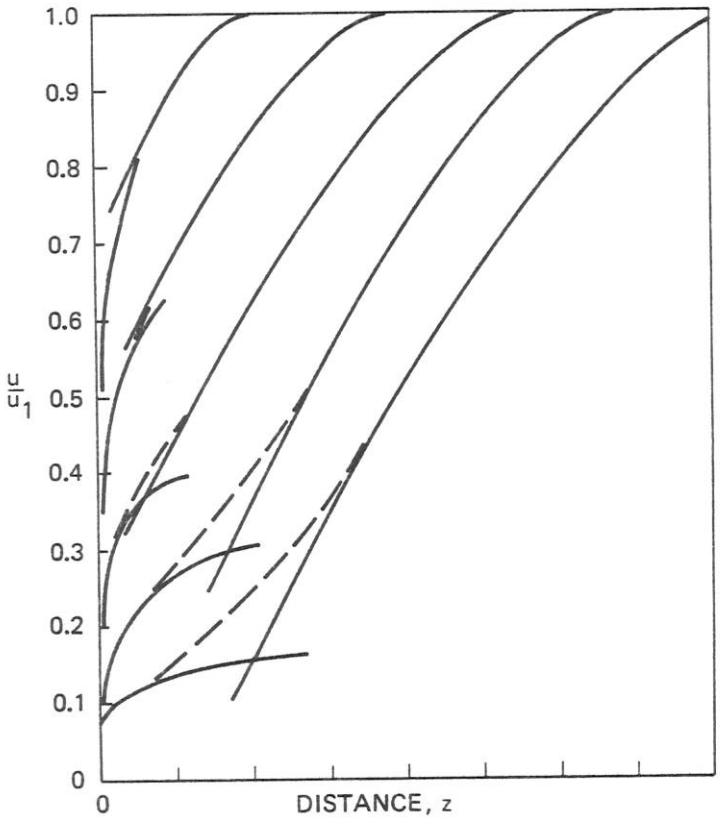

Fig. 6.18. Typical Boundary-Layer Profiles Illustrative of Blending Region, after Ross (1956)

outer regions blend for a number of typical velocity profiles. In some instances the functions for the two major turbulent regions seem to overlap and blending is unnecessary. However, for profiles that have large momentum deficiencies blending may occur through as much as 20% of the boundary layer.

Boundary layers on smooth plates in parallel flows having zero pressure gradients grow quite slowly and have outer turbulent regions which bear a constant relation to their inner regions. Clauser (1956) has called these *equilibrium boundary layers*. Unfortunately, most published boundary-layer analyses treat all boundary layers as though they were equilibrium layers. Not only

does this lead to serious errors regarding the mean flow, but also, as will be discussed, it leads to erroneous results concerning turbulent boundary-layer noise. It is essential that the spatial history extending over an upstream distance of about 50 boundary-layer thicknesses be taken into account.

Boundary-Layer Friction

The drag which a body experiences due to its boundary layer can be expressed in terms of a dimensionless friction coefficient, c_f, defined by

$$c_f \equiv \frac{\tau_w}{\frac{1}{2}\rho_o u_1^2} = 2\left(\frac{u_\tau^*}{u_1}\right)^2 . \tag{6.103}$$

As shown by Ross (1953, 1956), this friction coefficient is a function of a Reynolds number, R_θ, defined in terms of the local momentum thickness,

$$R_\theta \equiv \frac{\theta u_1}{\nu} , \tag{6.104}$$

and the effective velocity, u_θ, at a distance out from the wall equal to the momentum thickness. Thus, the law of the wall can be written

$$\frac{u_\theta}{u_1} = \frac{u_\tau^*}{u_1}\left[5.6 + 5.6 \log\left(\frac{u_\tau^*}{u_1} R_\theta\right)\right] , \tag{6.105}$$

the solution of which is approximately

$$\frac{u_\tau^*}{u_1} = \sqrt{\frac{c_f}{2}} \doteq \frac{u_\theta}{u_1}\left[0.7 + 5.0 \log\left(\frac{u_\theta}{u_1} R_\theta\right)\right]^{-1} . \tag{6.106}$$

From his study of several hundred velocity profiles, Ross (1956) found

$$\frac{u_\theta}{u_1} \doteq 0.885 - \frac{3}{5} D . \tag{6.107}$$

It follows that the friction coefficient for a smooth wall is a function of both the local momentum-thickness Reynolds number and previous history of the flow, as expressed by D or an equivalent parameter.

The above relations apply only to walls that are hydraulically smooth, i.e., any roughnesses are smaller than the thickness of the laminar sublayer. Walls having larger roughnesses are called hydraulically rough. For such walls, the laminar sublayer is thicker than it would be for a smooth wall since turbulent motions cannot penetrate into the roughness region. As discussed by Hama (1954), the logarithmic and linear curves for a hydraulically rough wall intersect at a value of $z = \epsilon$ related to the roughness heights and type. It follows that

$$\frac{u}{u_\tau^*} = \frac{\epsilon u_\tau^*}{\nu} + 5.6 \log \frac{z}{\epsilon} \tag{6.108}$$

in the inner turbulent region of rough boundary layers. It also follows that the skin friction coefficient is higher than for a smooth wall by an amount that depends on the ratio of $\epsilon u_\tau^*/\nu$ to 11.5.

Boundary-Layer Turbulence

The basic equations for viscous flows are the continuity equation and the Navier-Stokes form of the momentum equation. These were extended to turbulent conditions by Reynolds (1895), who assumed that instantaneous velocities could be expressed as the sum of time-independent mean values and fluctuating components in much the same manner as in Section 2.2 in deriving the acoustic wave equation. Reynolds found that the turbulent stress is given by

$$\tau_{ij} \doteq \left| \rho_o \overline{u_i' u_j'} \right| , \tag{6.109}$$

which relation was used by Lighthill in deriving Eq. 3.16 for turbulence noise sources. The turbulent stresses in a boundary layer can also be related to the velocity gradient through a length scale, ℓ, called the mixing length:

$$\tau = \left| \rho_o \ell^2 \left(\frac{\partial u}{\partial z} \right)^2 \right| . \tag{6.110}$$

It follows that the level of turbulence is proportional to the product of the mixing length and the velocity gradient.

The 3/2-power velocity deficiency relation, Eq. 6.102, is consistent with the assumptions of constant mixing length and linear dependence of shear stress in the outer region, as indicated in Fig. 6.17. Thus, expressing τ by

$$\tau(z) = \tau_o \left(1 - \frac{z}{\delta} \right) , \tag{6.111}$$

it follows that

$$\frac{du}{dz} = \frac{\sqrt{\tau_o/\rho_o}}{\ell} \sqrt{1 - \frac{z}{\delta}} = \frac{u_{\tau_o}^*}{\ell} \sqrt{1 - \frac{z}{\delta}} \tag{6.112}$$

and that

$$\frac{u}{u_1} = 1 - \frac{2}{3} \frac{\delta u_{\tau_o}^*}{\ell u_1} \left(1 - \frac{z}{\delta} \right)^{3/2} . \tag{6.113}$$

Comparing with Eq. 6.102, the magnitude of the deficiency, D, is related to the turbulence level

by

$$D = \frac{2}{3}\,\frac{\delta}{\ell}\,\frac{u^*_{\tau_o}}{u_1} \approx \frac{\delta}{\ell}\sqrt{\frac{\overline{u'v'}}{u_1^2}} \qquad (6.114)$$

Both the turbulence level and the scale of the eddies in the outer region are dependent on upstream history. Since the mixing length is roughly proportional to the boundary-layer thickness and since this thickness is close to that of an equilibrium boundary layer, it follows that the velocity deficiency is primarily controlled by the level of turbulence generated upstream. Figure 6.19 shows a typical shear stress distribution in which the local wall shear stress, τ_w, is significantly lower than the effective value, τ_o, that describes the outer region.

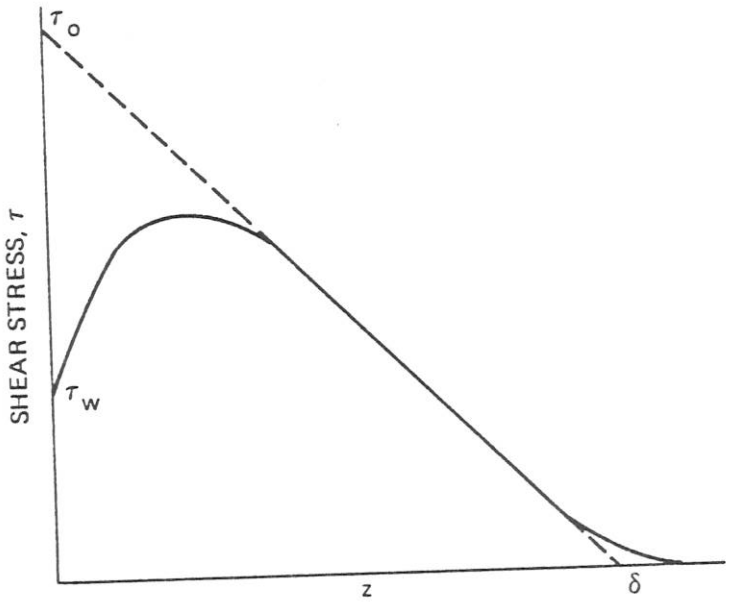

Fig. 6.19. Typical Shear Stress Distribution, from Ross (1956)

For boundary layers on flat plates with zero pressure gradients, τ_o is related to τ_w and a single universal velocity can be derived in terms of u^*_τ. The boundary-layer turbulence level can in this case be related to the wall shear stress. However, such relationships between boundary-layer turbulence levels and local wall shear stress coefficients are applicable only when equilibrium conditions exist.

Intermittency Effects

Equation 6.109 pertains to average turbulence levels in a turbulent flow. Actual turbulent shear flows are characterized by certain large scale phenomena that are called *intermittencies* to distinguish them from the smaller scale turbulent motions. These occur in both the outer and inner regions of a boundary layer. Corrsin and Kistler (1955) reported that the outer edge of a free turbulent shear flow is an irregular surface dividing non-turbulent from turbulent regions. The scale of the waviness is close to half the boundary-layer thickness. Thus, an instrument sensitive to turbulence placed in the outer part of a boundary layer will find itself in a turbulent field only

part of the time, the percentage decreasing from 100% at $z \approx \delta/3$ to zero somewhat beyond the apparent boundary-layer thickness.

A second important intermittent effect was discovered by Kline et al (1967), who found evidence of semi-periodic eddy formation in the laminar buffer zone involving large-scale spanwise motions and explosive bursts of turbulence into the turbulent zone. Streaks of vorticity preceding the bursts were photographed and were found to move at speeds close to 13.8 u_τ^*. The importance of this phenomenon was recognized by Black (1966) and by Landahl (1975). The latter concluded that these explosive bursts are a dominant source of high-frequency boundary-layer flow noise.

Wall Pressure Fluctuations

Many boundary-layer noise investigations of the past 20 years have concentrated on measuring various properties of wall pressure fluctuations associated with turbulent boundary layers on flat plates and in pipes. The results have been presented as fluctuation spectra and spatial correlations. As shown in Fig. 6.20, pressure fluctuation spectra sometimes peak at a non-dimensional fre-

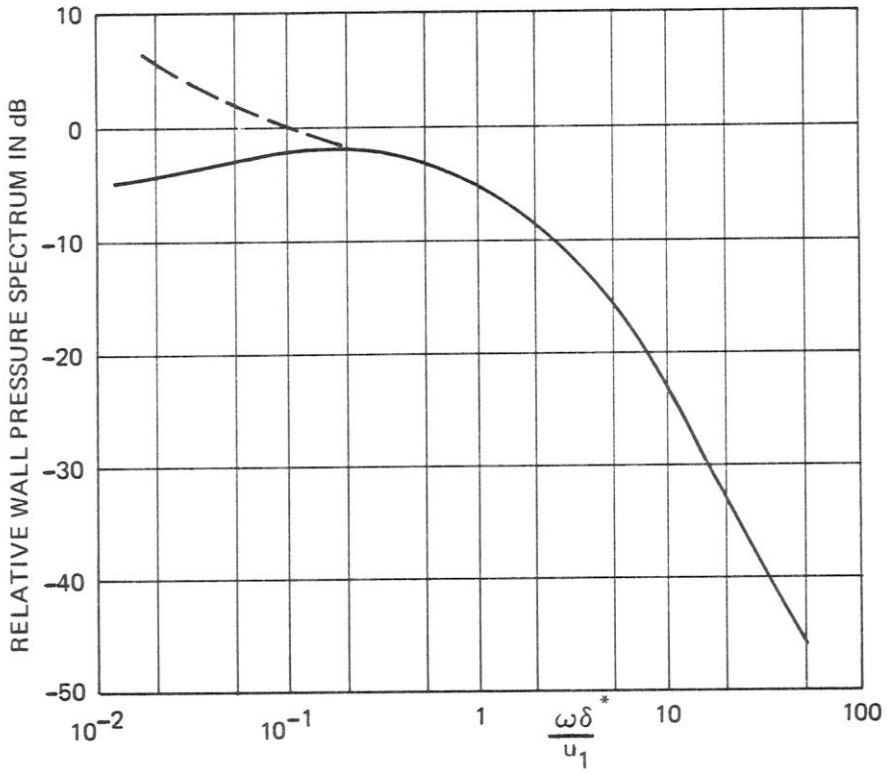

Fig. 6.20. Typical Wall Pressure Fluctuation Spectrum

quency ratio of about 0.2. They decrease markedly at higher frequencies by as much as 9 to 12 dB/octave. Moreover, as calculated by Corcos (1963, 1967) and confirmed by Gilchrist and Strawderman (1965), Lyamshev and Salosina (1966) and Geib (1967, 1969), measured high-frequency spectra are frequently affected by cancellation effects due to finite transducer size. Low-frequency spectra show a great deal of scatter, primarily due to extraneous noises but also due to actual differences of the test configurations.

The total wall pressure is dominated by low-frequency components and therefore is not much affected by transducer size. For equilibrium boundary layers with zero pressure gradient,

$$p_{rms} \approx 3c_f q_1 \approx 0.005 q_1 \ , \tag{6.115}$$

where

$$q_1 \equiv \frac{1}{2} \rho_o u_1^2 \ . \tag{6.116}$$

Different measurements have shown appreciable scatter for this quantity. Also, Mugridge (1971) found that wall pressures in the adverse pressure gradient region of a lifting airfoil are as much as 15 dB higher than those for a flat plate. Schloemer (1967) also found that the spectral distribution of pressure fluctuations is affected by favorable as well as adverse pressure gradients.

Longitudinal correlation measurements show that turbulence is convected by the mean flow. As would be expected, low-frequency components associated with larger eddies in the outer flow are convected at higher speeds than are higher-frequency, small-scale components. Typically, the convection velocity, u_c, for low-frequency components is about 80 to 85% of the free-stream flow speed while for the highest frequency components the ratio is only 60 to 65%.

Since turbulent pressure fluctuations are dependent on turbulence levels which in turn are related to hydrodynamic drag through the wall shear stress, it would be expected that anything that could be done to reduce drag would also reduce pressure fluctuations. Kadykov and Lyamshev (1970) confirmed that the addition of dilute polymer solutions reduces pressure fluctuations by from 1 to 8 dB. This reduction of pressure fluctuations is related to the drag reduction first reported by Toms (1948) and more recently confirmed by Fabula (1965), Van Driest (1970) and many others.

Self-Noise of Flush-Mounted Hydrophones

One form of flow noise is that of flush-mounted hydrophones under a turbulent boundary layer. For such hydrophones, wall pressure fluctuations, sometimes referred to as *pseudo-sound*, are usually the dominant source of self-noise. The pseudo-sound component of the self-noise spectrum is given by the product of the pressure spectrum, as depicted in Fig. 6.20, and the hydrophone size cancellation spectrum; it therefore depends on the ratio of hydrophone size to boundary-layer thickness as well as on the dimensionless frequency.

At the lowest frequencies, hydrophone size effects are negligible and the pressure spectrum is approximately flat. As mentioned above, measurements in this frequency regime show considerable scatter depending on test configuration. However, as summarized by Haddle and Skudrzyk (1969) and by Blake (1970), the wall pressure spectrum can be estimated within a factor of two from

$$p'(\omega) \approx 0.003 \rho_o u_1^{3/2} \delta^{*1/2} \ . \tag{6.117}$$

Thus, low-frequency self-noise levels increase with boundary-layer thickness as well as with flow speed.

For somewhat higher frequencies, most measurements display a negative slope of about 9 dB/octave for about two decades of frequency. For this part of the spectrum, Lyamshev and

Salosina (1966) found

$$p'(\omega) \doteq 0.003\rho_o u_c^{3/2} a^{1/2} \left(\frac{u_c}{\omega a}\right)^{3/2} \left(\frac{\delta^*}{a}\right)^{3/4} . \qquad (6.118)$$

At a given frequency in this part of the spectrum, self-noise increases with the cube of flow speed.

At high frequencies the hydrophone size cancellation effect adds to the spectral slope of the turbulent fluctuations and produces a very rapid decrease of pseudo-sound flow noise. However, flow noise measurements by Skudrzyk and Haddle (1960) showed no such trend. In a later article, Haddle and Skudrzyk (1969) stressed the importance of directly radiated turbulence noise from the boundary layer itself and proposed that such acoustic noise dominates relative to pseudo-sound at the higher frequencies.

Hydrophone shape is important in the frequency region for which flow noise is dominated by pseudo-sound. The dimension which controls in Eq. 6.118 is that in the direction of motion of the flow. Thus, White (1967) has reported reductions of self-noise levels of up to 8 dB by using rectangular and elliptical transducers with their longest dimensions in the direction of flow. These lower flow noise levels in the pseudo-sound regime are associated with the fact that turbulent eddies are convected across the transducer face at a relatively slow speed. Defining a turbulent hydrodynamic wave number, k_t, as the ratio of the angular frequency to the convection wave speed, i.e.,

$$k_t \equiv \frac{\omega}{u_c} , \qquad (6.119)$$

one can interpret White's result as the reduction of response of a continuous line array having $kL > 1$, analogous to that for acoustic waves as derived in Section 4.7.

Arrays of Flush-Mounted Hydrophones

Just as an array of point transducers can be used in place of a continuous line as a spatial filter for acoustic waves, so an array of small transducers can be used to discriminate against turbulent pressure fluctuations. Jorgensen and Maidanik (1968) compared the filtering action of systems of two and three elements with that of a continuous line, finding equally good discrimination for the discrete systems provided $k_t d < 2$, where d is the separation of the elements. Maidanik (1967) considered a larger number of elements and pointed out that the response could be altered by steering the array, i.e., by introducing phase shifts between the elements. More recently, Kennedy (1975) has shown that optimum beam-forming techniques can be used to design transducer arrays having maximum discrimination against turbulent pressure fluctuations while still having full sensitivity to sonic signals.

Maidanik and Jorgensen (1967) proposed the use of an even-number array of alternating polarity transducers as a system that would be insensitive to acoustic disturbances but would respond to turbulent fluctuations obeying certain relations between wave number and frequency. Such a system, which they termed a *wave-vector filter*, is analogous to a diffraction grating in optics. Its purpose is to study boundary-layer pressure fluctuations without interference from acoustic components of the flow noise. Blake and Chase (1971) applied wave-vector filters to a series of boundary-layer measurements, finding them useful in suppressing wind-tunnel background noise. Wave-vector filters are particularly valuable when making measurements of convection speed as a function of frequency.

Radiated Flow Noise

There are several basic physical mechanisms by which noise may be radiated from turbulent boundary layers. Controversy concerning their relative importance has pervaded the literature on this subject and the evidence does not solidly establish any one mechanism as dominant. Furthermore, the effectiveness of any of them is often dependent on secondary factors. It seems likely that in any given situation several physical mechanisms may contribute to the total noise field.

One source of radiated noise from any turbulent fluid motion is the direct quadrupole radiation from the turbulent stresses treated by Lighthill and discussed in Section 3.4. However, this radiation is strongly dependent on Mach number and is negligible at the low Mach numbers of liquid flows. Curle (1955) showed that in the presence of a rigid boundary fluctuating shear stresses can produce dipole radiation associated with the resultant wall pressure fluctuations. Powell (1960) noted that when the wall is planar, rigid and large compared to a wavelength these dipole components tend to cancel and in this case the only effect of the boundary is to augment the quadrupole radiation by a factor of four. More recently, Landahl (1975) reexamined this question in light of the discovery by Kline et al (1967) of turbulence bursts in the laminar buffer region. Landahl showed that the intensity of dipole radiation associated with these bursts is

$$I \sim \tau_w u_\tau^* \left(\frac{u_\tau^*}{c_o} \right)^3 S = \rho_o u_1^3 \left(\frac{c_f}{2} \right)^3 M^3 S \,. \tag{6.120}$$

Since c_f varies with flow speed approximately as $u_1^{-1/5}$, this direct radiation can be expected to vary with flow speed to approximately the 5.4 power.

Haddle and Skudrzyk (1969) measured the noise radiated by metal shell and solid wood buoyant bodies of torpedo shape. Their measured levels were independent of body construction, from which they concluded that direct radiation from the turbulence was the dominant mechanism. However, other (unpublished) results indicate that noise radiated by buoyant bodies may come from the stabilizing fins rather than from the body itself. Since the same fins were used on both models, the Haddle and Skudrzyk results cannot be said to prove conclusively that rigid-wall turbulence radiation is dominant.

The mechanism that has received the most attention is that of excitation of flexural vibrations by wall pressure fluctuations and radiation by these vibrations. Evidence that this mechanism can be a dominant one was found by Ludwig (1962) and Maestrello (1965). Both investigators measured the noise radiated by rectangular panels in wind tunnels, finding roughly fifth-power dependencies on flow speed and inverse variation of radiated acoustic power with plate thickness.

While several theoretical analyses of flow noise involving wall flexural vibrations have been made, none can be said to be consistently in good agreement with experimental results. Most of the turbulent energy is convected at speeds that are low compared to the speeds of both plate flexural waves and sound in the acoustic medium. As a result, all but a very small fraction of the vibratory energy induced in the plate by the turbulence is in non-radiating modes. Radiation can only occur from that very small fraction of the turbulent energy that is in the very low wave number part of the spectrum and from any of the higher wave number vibratory components that are converted to low wave numbers through scattering by ribs, supports and other discontinuities.

The first attempt to calculate radiated flow noise involving plate flexural vibrations was made by Dyer (1958, 1959). He found that the mean-square plate vibration is independent of turbulence convection speed when that speed is small compared to the speed of flexural waves, as is true for liquids. Dyer also predicted that plate damping would be an effective method of reducing flow

noise. A similar analysis by Aupperle and Lambert (1973) for thin plates gave results in good agreement with experimental data reported by Ludwig (1962). White (1966) and Davies (1971) applied modal analyses treating corner as well as edge modes to derive formulas for the radiated flow noise of thin panels in air. Their results also appear to be in good agreement with thin panel experimental measurements. Davies found that fluid loading effects can reduce radiated flow noise levels from thin panels by as much as 10 to 15 dB.

Turbulent pressure fluctuations seem clearly to excite structural vibrations in non-rigid walls. Strawderman and Brand (1969) and others have successfully calculated these vibrations using measured wall pressure spectra and Corcos' (1964) results for cross-power spectral densities. The degree to which these vibrations radiate and the ratio of their radiation to rigid-wall dipole radiation remain unknown. The author agrees with Vecchio and Wiley (1973), who concluded that flexural wave radiation is usually dominant at low frequencies while direct dipole radiation is often stronger at the higher frequencies.

Domed Sonar Self-Noise

In order to avoid the direct pseudo-sound noise of turbulent boundary-layer pressure fluctuations, most sonar receivers are located inside thin domes that isolate them from the turbulence while transmitting acoustic signals virtually undistorted. The turbulence is then on the other side of the structure from the receiver, and flexural vibrations and their radiation must be the dominant mechanism whereby flow noise is received. Analyses of this case have been published by Dyer (1958), Plakhov (1966), Maidanik (1968) and Dowell (1969, 1970). Dyer attempted a complete analysis of both vibration excitation and cavity radiation aspects of the problem but was forced for lack of sufficient information to make a number of simplifying assumptions. He noted that coincidence may occur within the frequency range of interest and that radiation should be treated differently in the two frequency regimes. Plakhov treated the problem in a manner similar to that of transmission through a wall placed between two fluids having respective wave speeds of u_c and c_o. He concluded that those structural properties which increase the TL of a wall also tend to decrease turbulent flow noise. In agreement with this conclusion, Maidanik noted that ribs and other discontinuities that increase radiation of flexural waves from plates also increase the transmission of turbulence noise. Dowell included the effects of non-linear plate stiffness and cavity fluid motions, finding that flutter can occur in some cases when the panel is very thin.

In summary, while no single, simple formulation is available, it appears that domes do indeed reduce flow noise levels in most cases, and that dome design should follow the principles of good wall design by avoiding discontinuities that can act to transform vibrations from high wave number, non-radiating modes into low wave number, radiating modes.

REFERENCES

Sections 6.1-6.4

Blake, W.K., The acoustic radiation from unbaffled strips with application to a class of radiating panels, *J. Sound and Vibr., 39*, 77-103, 1975.

Blank, F.G., Sound field near a vibrating elastic plate, *Sov. Phys.-Acoustics, 14*, 31-36, 1968.

Brekhovskikh, L.M., Propagation of flexural waves in plates, *J. Tech. Phys. (USSR), 14*, 9, 568-576, 1955 (in Russian).

Cremer, L., Theorie der Schalldämmung dunner Wände bei Schragen Einfall, *Akustische Zeit., 7*, 81-104, 1942.

Cremer, L., The Propagation of Structure-Borne Sound, *Dept. of Scientific and Indust. Res. (London) Sponsored Res., Rept. Ser. B*, No. 1, 1950; also, *Acustica, 3*, 317-335, 1953.

Cremer, L., Heckl, M. and Ungar, E.E., *Structure-Borne Sound*, Springer-Verlag, New York, 1973 (Chapters 4 and 6).

Crighton, D.G., Force and momentum admittance of plates under arbitrary fluid loading, *J. Sound and Vibr., 20*, 209-218, 1972.

Donaldson, J.M., Reduction of noise radiated from ship structures, *Applied Acoustics, 1*, 275-291, 1968.

Dyer, I., Moment impedance of plates, *J.A.S.A., 32*, 1290-1297, 1960.

Feit, D., Pressure radiated by a point-excited elastic plate, *J.A.S.A., 40*, 1489-1494, 1966.

Feit, D., Sound radiation from orthotropic plates, *J.A.S.A., 47*, 388-389, 1970.

Franken, P.A., Input impedances of simple cylindrical structures, *J.A.S.A., 32*, 473-477, 1960.

Gösele, K., Radiation from plates excited into bending vibrations, *Acustica, 3*, 243-248, 1953; *6*, 94-98, 1956 (in German).

Gutin, L. Ya, Sound radiation from an infinite plate excited by a normal point force, *Sov. Phys.-Acoustics, 10*, 369-371, 1964.

Heckl, M., Radiation from point-excited plates, *Acustica, 9*, 371-380, 1959 (in German).

Heckl, M., Investigation of orthotropic plates, *Acustica, 10*, 109-115, 1960 (in German).

Heckl, M., Wave propagation of beam-plate systems, *J.A.S.A., 33*, 640-651, 1961.

Heckl, M., Vibrations of point-driven cylindrical shells, *J.A.S.A., 34*, 1553-1557, 1962.

Heckl, M., Radiation from a point-excited plate in water, *Acustica, 13*, 182, 1963 (in German).

Howe, M.S. and Heckl, M., Sound radiation from plates with density and stiffness discontinuities, *J. Sound and Vibr., 21*, 193-203, 1972.

Junger, M.C., "Structure-Borne Noise," in *Structural Mechanics*, Pergamon Press, Oxford, 1960.

Junger, M.C. and Feit, D., *Sound, Structures and Their Interaction*, M.I.T. Press, Cambridge, Mass., 1972 (Chapters 5 to 8 and 10).

Junger, M.C., Radiation and scattering by submerged elastic structures, *J.A.S.A., 57*, 1318-1326, 1975.

Kinsler, L.E. and Frey, A.R., *Fundamentals of Acoustics*, 2nd Edit., Wiley, New York, 1962 (Chapter 4).

Komarova, L.N., Radiation from shells, *Sov. Phys.-Acoustics, 15*, 332-335, 1969.

Kurtze, G. and Bolt, R.H., On the interaction between plate bending waves and their radiation load, *Acustica, 9*, Beihefte 1, 238-242, 1959.

Lyapunov, V.T., Flexural wave propagation in a liquid-loaded plate with an obstruction, *Sov. Phys.-Acoustics, 14*, 353-355, 479-482, 1968.

Lyon, R.H., Sound radiation from a beam attached to a plate, *J.A.S.A., 34*, 1265-1268, 1962.

Maidanik, G., Response of ribbed panels to reverberent acoustic fields, *J.A.S.A., 34*, 809-826, 1962.

Maidanik, G., The influence of fluid loading on the radiation from orthotropic plates, *J. Sound and Vibr., 3*, 288-299, 1966.

Maidanik, G. and Kerwin, E.M., Jr., Influence of fluid loading on the radiation from infinite plates below the critical frequency, *J.A.S.A., 40*, 1034-1038, 1966.

Maidanik, G., Vibrational and radiative classifications of modes of a baffled finite panel, *J. Sound and Vibr., 34*, 447-455, 1974.

Manning, J.E. and Maidanik, G., Radiation properties of cylindrical shells, *J.A.S.A., 36*, 1691-1699, 1964.

Mindlin, R.D., Influence of rotatory inertia and shear on flexural motions of isotropic elastic plates, *J. Appl. Mech., 18*, 31-38, 1951.

Morse, P.M. and Ingard, K.U., *Theoretical Acoustics*, McGraw-Hill, New York, 1968 (Chapter 10).

Nelson, H.M., A universal dispersion curve for flexural wave propagation in plates and bars, *J. Sound and Vibr., 18*, 93-100, 1971.

Nikiforov, A.S., Radiation from a plate of finite dimensions with arbitrary boundary conditions, *Sov. Phys.-Acoustics, 10*, 178-182, 1964.

Nikiforov, A.S., Vibration reduction of a single reinforcing beam, *Sov. Phys.-Acoustics, 15*, 541-542, 1969.

Plakhov, D.D., Sound field of a multispan plate, *Sov. Phys.-Acoustics, 13*, 506-510, 1967.

Rayleigh, Lord, *Theory of Sound*, Vol. I, Dover, New York, 1945 (Chapters 10 and 10A).

Romanov, V.N., Radiation of sound by an infinite plate with reinforcing beams, *Sov. Phys.-Acoustics, 17*, 92-96, 1971, and *18*, 490-493, 1972.

Rybak, S.A. and Tartakovskii, B.D., On the vibrations of thin plates, *Sov. Phys.-Acoustics, 9*, 51-55, 1963.

Skudrzyk, E.J., Kautz, B.R. and Greene, D.C., Vibration of, and bending-wave propagation in plates, *J.A.S.A., 33*, 36-45, 1961.

Skudrzyk, E., *Simple and Complex Vibratory Systems*, The Pennsylvania State University Press, University Park, Pa., 1968 (Chapters 8, 9, 12 and 14).

Smith, P.W., Jr., Coupling of sound and panel vibration below the critical frequency, *J.A.S.A., 36*, 1516-1520, 1964.

Snowdon, J.C., Forced vibration of internally damped rectangular and square plates, *J.A.S.A., 56*, 1177-1184, 1974.

Szechenyi, E., Modal densities and radiation efficiencies of unstiffened cylinders using statistical methods, *J. Sound and Vibr., 19*, 65-81, 83-94, 1971.

Ungar, E.E., Transmission of plate flexural waves through reinforcing beams, *J.A.S.A., 33*, 633-639, 1961.

Ver, I.L. and Holmer, C.I. "Interaction of Sound Waves with Solid Structures," Chapter 11 in *Noise and Vibration Control*, L.L. Beranek (Ed.), McGraw-Hill, New York, 1971 (pp. 270-357).

Westphal, W., Radiation of flexurally excited walls, *Acustica, 4*, 603-610, 1954 (in German).

Yaneske, P.P., A restatement of the principle of coincidence and resonance, *J. Sound and Vibr., 25*, 51-73, 1972.

Section 6.5

Beranek, L.L., The transmission and radiation of acoustic waves by structures, *J. Inst. Mech. Engin., 6*, 162-169, 1959; also, Chapter 13 of *Noise Reduction*, L.L. Beranek (Ed.), McGraw-Hill, New York, 1960.

Cremer, L., Heckl, M. and Ungar, E.E., *op. cit.* (Chapter 6).

Crocker, M.J. and Price, A.J., Sound transmission using statistical energy analysis, *J. Sound and Vibr., 9*, 469-486, 1969.

Heckl, M., Several applications of the reciprocity principle in acoustics, *Frequenz, 18*, 299-304, 1964 (in German).

Kinsler, L.E. and Frey, A.R., *op. cit.* (Chapter 6).

Kurtze, G., Bending wave propagation in multilayer plates, *J.A.S.A., 31*, 1183-1201, 1959.

Kurtze, G. and Watters, B.G., New wall design for high transmission loss or high damping, *J.A.S.A., 31*, 739-748, 1959.

Kurtze, G., *Physik und Technik der Lärmbekämpfung*, G. Braun, Karlsruhe, 1964 (Chapters 4 and 5).

Lyamshev, L.M., A question in connection with the principle of reciprocity in acoustics, *Sov. Phys.-Doklady, 4*, 406-409, 1959.

Plakov, D.D., Transmission of a sound wave through a laminated plate reinforced with stiffness members, *Sov. Phys.-Acoustics, 14*, 67-70, 1968.

Richards, E.J. and Mead, D.J. (Ed.), *Noise and Acoustic Fatigue in Aeronautics*, John Wiley, London, 1968 (Chapters 3 and 23).

Schiller, K.K., Physical aspects of sound insulation through walls, *J. Sound and Vibr., 6*, 283-295, 1967.

Shenderov, E.L., Transmission of sound through a thin plate with interjacent supports, *Sov. Phys.-Acoustics, 9*, 289-294, 1963.

Shenderov, E.L., Sound transmission through a thin supported plate, *Sov. Phys.-Acoustics, 10*, 187-190, 1964.

Shenderov, E.L., Relationship of sound radiation by plates to their acoustic transmissivity, *Sov. Phys.-Acoustics, 12*, 336-338, 1966.

Smith, P.W., Jr., *op. cit.*, 1964.

Venzke, G., Dämmig, P. and Fischer, H.W., Influence of stiffeners on the sound radiation and transmission loss of metal walls, *Acustica, 29*, 29-40, 1973 (in German).

Ver, I.L. and Holmer, C.I., *op. cit.* (1971).

Warren, W.E., Low-frequency power radiation from a flat plate into an acoustic fluid, *J.A.S.A., 56*, 1764-1769, 1974.

White, P.H. and Powell, A., Transmission of random sound and vibration through a rectangular double wall, *J.A.S.A., 40*, 821-832, 1966.

Young, J.E., Transmission of sound through thin elastic plates, *J.A.S.A., 26*, 485-492, 1954.

Section 6.6

Aupperle, F.A. and Lambert, R.F., Effects of roughness on measured wall-pressure fluctuations beneath a turbulent boundary layer, *J.A.S.A., 47*, 359-370, 1970.

Aupperle, F.A. and Lambert, R.F., Acoustic radiation from plates excited by flow noise, *J. Sound and Vibr., 26*, 223-245, 1973.

Black, T.J., "Some Practical Applications of a New Theory of Wall Turbulence," Paper 21 in *Proc. 1966 Heat Transfer and Fluid Mechanics Institute*, Stanford University Press, 1966 (pp. 366-386).

Blake, W.K., Turbulent boundary-layer wall pressure fluctuations on smooth and rough walls, *J. Fluid Mech., 44*, 637-660, 1970.

Blake, W.K. and Chase, D.M., Wave number-frequency spectra of turbulent-boundary-layer pressure measured by microphone arrays, *J.A.S.A., 49*, 862-877, 1971.

Bull, M.K., Wall-pressure fluctuations associated with subsonic turbulent-boundary-layer flow, *J. Fluid Mech., 28*, 719-754, 1967.

Clauser, F.H., "The Turbulent Boundary Layer," in *Advances in Applied Mechanics*, Vol IV, Academic Press, New York, 1956.

Coles, D., The law of the wake in the turbulent boundary layer, *J. Fluid Mech., 1*, 191-226, 1956.

Corcos, G.M., Resolution of pressure in turbulence, *J.A.S.A., 35*, 192-199, 1963.

Corcos, G.M., Structure of the turbulent pressure field in boundary-layer flows, *J. Fluid Mech., 18*, 353-378, 1964.

Corcos, G.M., The resolution of turbulent pressures at the wall of a boundary layer, *J. Sound and Vibr., 6*, 59-70, 1967.

Corrsin, S. and Kistler, A.L., Free-Stream Boundaries of Turbulent Flows, *N.A.C.A. Tech. Rept. 1244*, 1955.

Crighton, D.G. and Ffowcs Williams, J.E., Real space-time Green's functions applied to plate vibrations induced by turbulent flows, *J. Fluid Mech., 38*, 305-314, 1969.

Curle, N., The influence of solid boundaries upon aerodynamic sound, *Proc. Royal Soc. (London), A231*, 505-514, 1955.

Davies, H.G., Low-frequency random excitation of water-loaded rectangular plates, *J. Sound and Vibr., 15*, 107-126, 1971.

Davies, H.G., Sound from turbulent-boundary-layer-excited panels, *J.A.S.A., 49*, 878-889, 1971.

Dowell, E.H., Transmission of noise from a turbulent boundary layer through a flexible plate into a closed cavity, *J.A.S.A., 46*, 238-252, 1969.

Dowell, E.H., Noise or flutter or both, *J. Sound and Vibr., 11*, 159-180, 1970.

Dyer, I., "Sound Radiation into a Closed Space from Boundary Layer Turbulence," *Proc. Second Symposium on Naval Hydrodynamics*, O.N.R. ACR-38, Washington, 1958 (pp. 151-174).

Dyer, I., Response of plates to a decaying and convecting random pressure field, *J.A.S.A., 31*, 922-928, 1959.

Fabula, A.G., "The Toms Phenomenon in the Turbulent Flow of Very Dilute Polymer Solutions," in *Proc. Fourth Inter. Congr. on Rheology*, Interscience Publ., New York, 1965 (pp. 455-479).

Ffowcs Williams, J.E., The influence of simple supports on the radiation from turbulent flow near a plane compliant surface, *J. Fluid Mech., 26*, 641-649, 1966.

Ffowcs Williams, J.R. and Hall, L.H., Aerodynamic sound generation by turbulent flow near a half plane, *J. Fluid Mech., 40*, 657-670, 1970.

Gardner, S., On surface pressure fluctuations produced by boundary layer turbulence, *Acustica, 16*, 67-74, 1965.

Geib, F.E., Jr., Measurements on the effect of transducer size on the resolution of boundary-layer pressure fluctuations, *J.A.S.A., 46*, 253-261, 1969.

Gilchrist, R.B. and Strawderman, W.A., Experimental hydrophone-size connection factor for boundary-layer pressure fluctuations, *J.A.S.A., 38*, 298-302, 1965.

Haddle, G.P. and Skudrzyk, E.J., The physics of flow noise, *J.A.S.A., 46*, 130-157, 1969.

Hama, F.R., Boundary-layer characteristics for smooth and rough surfaces, *Trans. Soc. of Naval Arch. and Marine Eng., 62*, 333-358, 1954.

Hoyt, J.W. and Fabula, A.G., "The Effect of Additives on Fluid Friction," *Proc. Fifth Symposium on Naval Hydrodynamics*, O.N.R. ACR-112, Washington, 1964 (pp. 947-974).

Jorgensen, D.W. and Maidanik, G., Response of a system of point transducers to turbulent boundary-layer pressure field, *J.A.S.A., 43*, 1390-1394, 1968.

Kadykov, I.F. and Lyamshev, L.M., Influence of polymer additives on the pressure fluctuations in a boundary layer, *Sov. Phys.-Acoustics. 16*, 59-63, 1970.

Kennedy, R.M., Cancellation of turbulent boundary-layer pressure fluctuations, *J.A.S.A., 57*, 1062-1066, 1975.

Kline, S.J., Reynolds, W.C., Schraub, F.A. and Runstadler, P.W., The structure of turbulent boundary layers, *J. Fluid Mech., 30*, 741-773, 1967.

Landahl, M.T., Wave mechanics of boundary-layer turbulence and noise, *J.A.S.A., 57*, 824-831, 1975.

Leehey, P., "Trends in Boundary Layer Noise Research," in *Aerodynamic Noise*, H.S. Ribner (Ed.), University of Toronto Press, Toronto, 1969.

Lilley, G.M., Pressure Fluctuations in an Incompressible Turbulent Boundary Layer, *Cranfield College of Aero. Rept. 133*, June 1960.

Ludwieg, H., Instrument for measuring the wall shearing stress of turbulent boundary layers, *Ing.-Archiv, 17*, 207-218, 1949; translated in *N.A.C.A. Tech. Memo 1284*, 1950.

Ludwieg, H. and Tillmann, W., Investigation of the wall shearing stress in turbulent boundary layers, *Ing.-Archiv, 17*, 288-299, 1949; translated in *N.A.C.A. Tech. Memo 1285*, 1950.

Ludwig, G.R., An Experimental Investigation of the Sound Generated by Thin Steel Panels Excited by Turbulent Flow, *Univ. of Toronto, Inst. for Aero. Studies Rept. 87*, Nov. 1962.

Lyamshev, L.M., Analysis of acoustic radiation from a turbulent aerodynamic flow, *Sov. Phys.-Acoustics, 6*, 472-476, 1960.

Lyamshev, L.M. and Solosina, S.A., Influence of pickup dimensions on measurement of the spectrum of wall pressure fluctuations in a boundary layer, *Sov. Phys.-Acoustics, 12*, 228-229, 1966.

Maestrello, L., Measurement of noise radiated by boundary-layer excited panels, *J. Sound and Vibr., 2*, 100-115, 270-292, 1965.

Maestrello, L., Use of a turbulent model to calculate the vibration and radiation responses of a panel, *J. Sound and Vibr., 5*, 407-448, 1967.

Maidanik, G., Flush-mounted pressure transducer systems as spatial and spectral filters, *J.A.S.A., 42*, 1017-1024, 1967.

Maidanik, G. and Jorgensen, D.W., Boundary wave-vector filters for the study of the pressure field in a turbulent boundary layer, *J.A.S.A., 42*, 494-501, 1967.

Maidanik, G., Domed sonar system, *J.A.S.A., 44*, 113-124, 1968.

Mugridge, B.D., Turbulent boundary layers and surface pressure fluctuations on two-dimensional aerofoils, *J. Sound and Vibr., 18*, 475-486, 1971.

Plakhov, D.D., Sound field of an infinite plate acted upon by random pressure fluctuations, *Sov. Phys.-Acoustics, 12*, 415-418, 1966.

Powell, A., Aerodynamic noise and the plane boundary, *J.A.S.A., 32*, 982-990, 1960.

Prandtl, L., "The Mechanics of Viscous Fluids," in Vol. 3 of *Aerodynamic Theory*, W.F. Durand (Ed.), Julius Springer, Berlin, 1935.

Reynolds, O., On the dynamical theory of incompressible viscous fluids, *Phil. Trans. Royal Soc. (London), A186*, 123-164, 1895.

Richards, E.J. and Mead, D.J. (Ed.), *Noise and Acoustic Fatigue in Aeronautics*, John Wiley, London, 1968 (Chapters 8, 14 and 15).

Ross, D. and Robertson, J.M., Shear stress in a turbulent boundary layer, *J. Appl. Phys., 21*, 557-561, 1950.

Ross, D. and Robertson, J.M., A superposition analysis of the turbulent boundary layer in an adverse pressure gradient, *J. Appl. Mech., 18*, 95-100, 1951.

Ross, D., "A New Analysis of Nikuradse's Experiments on Turbulent Flow in Smooth Pipes," in *Proc. Third Midwestern Conf. on Fluid Mechanics*, Univ. of Minnesota, 1953; also *Ord. Res. Lab. Rept. 7958-246*, Sept. 1952.

Ross, D., A physical approach to turbulent-boundary-layer problems, *Trans. Am. Soc. Civil Engin., 121*, 1219-1254, 1956.

Schlichting, H., *Boundary-Layer Theory*, 6th Edit., McGraw-Hill, New York, 1968 (Chapters 3, 4, 18-22).

Schloemer, H.H., Effects of pressure gradients on turbulent-boundary-layer wall-pressure fluctuations, *J.A.S.A., 42*, 93-113, 1967.

Schubauer, G.B. and Tchen, C.M., *Turbulent Flow*, Princeton University Press, Princeton, 1959 (Chapter 4).

Schultz-Grunow, F., "Über das Nachwirken der Turbulenz bei örtlich und zeitlich verzögerter Grenzschichtströmung," *Proc. Fifth Inter. Cong. for Appl. Mech.*, Cambridge, Mass., 1938 (pp. 428-435).

Skudrzyk, E.J. and Haddle, G.P., Noise production in a turbulent boundary layer by smooth and rough surfaces, *J.A.S.A., 32*, 19-34, 1960; also *Proc. Second Symposium on Naval Hydrodynamics*, O.N.R. ACR-38, Washington, 1958 (pp. 75-105).

Strawderman, W.A. and Brand, R.S., Turbulent-flow-excited vibration of a simply supported rectangular flat plate, *J.A.S.A., 45*, 177-192, 1969.

Toms, B.A., "Some Observations on the Flow of Linear Polymer Solutions through Straight Tubes at Large Reynolds Numbers," in *Proc. Fifth Inter. Congr. on Rheology*, North Holland Publ. Co., Amsterdam, 1948 (pp. 135-141).

Townsend, A.A., Equilibrium layers and wall turbulence, *J. Fluid Mech., 11*, 97-120, 1961.

Van Driest, E.R., Turbulent drag reduction of polymeric solutions, *J. Hydronautics, 4*, 120-126, 1970.

Vecchio, E.A. and Wiley, C.A., Noise radiated from a turbulent boundary layer, *J.A.S.A., 53*, 596-601, 1973.

White, P.H., Transduction of boundary-layer noise by a rectangular panel, *J.A.S.A., 40*, 1354-1362, 1966.

White, P.H., Effect of transducer size, shape, and surface sensitivity on the measurement of boundary-layer pressures, *J.A.S.A., 41*, 1358-1363, 1967.

Willmarth, W.W. and Wooldridge, C.E., Measurements of the fluctuating pressure at the wall beneath a thick turbulent boundary layer, *J. Fluid Mech., 14*, 187-210, 1962; also *Univ. of Michigan Tech. Rept. 02920-2-T*, April 1962.

Willmarth, W.W. and Roos, F.W., Resolution and structure of the wall pressure field beneath a turbulent boundary layer, *J. Fluid Mech., 22*, 81-94, 1965.

Willmarth, W.W., Pressure fluctuations beneath turbulent boundary layers, *Ann. Rev. Fluid Mech., 7*, 13-38, 1975.